

CADOMIAN AND POST-CADOMIAN TECTONICS WEST OF THE RHODOPE MASSIF – THE FROLOSH GREENSTONE BELT AND THE OGRAZHDENIAN METAMORPHIC SUPERCOMPLEX

Ivan Zagorchev¹, Constantin Balica², Evgeniya Kozhoukharova¹,
Ioan Coriolan Balintoni², Gavril Săbău³, Elena Negulescu³

¹Bulgarian Academy of Sciences, Sofia, Bulgaria,

²University Babeș-Bolyai, Cluj-Napoca, Romania

³Geological Institute of Romania, Bucharest, Romania

i_zagorchev@geology.bas.bg

A b s t r a c t: The Frolosh Greenstone Belt (FGB) is traced at a distance of more than 200 km in the territories of Bulgaria, Macedonia and Serbia. It consists of various greenschist-facies rocks (actinolite schists, phyllites, calcareous schists, impure marbles, metasandstones, metadiabases, massive green rocks, etc.) of the Frolosh metamorphic complex with bodies of metabasites (including Iherzolites), and inliers (retrogressed mica gneisses and migmatites) from the Ograzhdenian supercomplex. The complex is intruded by bodies of gabbro (occasionally with ultramafic cumulates), diorites to granites (Struma diorite formation). U-Pb studies on zircons yielded Cadomian ages within the time span between c. 574 and 517 Ma. The Frolosh complex covers the ultrametamorphic (migmatized gneisses and amphibolites; tourmaline-biotite schists; quartzo-feldspathic gneisses; lensoid bodies of metaperidotites to norites) of the Ograzhdenian supercomplex. The Ograzhdenian rocks are intersected by diatectic metagranites overprinted by amphibolite-facies metamorphism. Dominant U-Pb ages vary between 470 and 430 Ma. The contact between the Frolosh complex and the Ograzhdenian supercomplex has been subject of long discussion and controversial interpretations. Now we emphasize on the multistage developments of both complexes as demonstrated both by field evidence and isotopic dating. The Ograzhdenian supercomplex has been subject of Precambrian tectonometamorphism witnessed by Rb-Sr whole-rock isochron data and relict U-Pb zircon data. Ordovician to Silurian anatectites (metatectic migmatization, diatexis) are intruded by Permo-Triassic granites. The contact between the Ograzhdenian supercomplex and the covering Frolosh complex is regarded as a thick complex zone of multistage tectonometamorphic development rather than a “razor-blade” surface of one-stage origin. As a boundary between suprastructure and infrastructure, it played an important role throughout the Phanerozoic, and acted as a screen with a steep thermal gradient during the Ordovician-Silurian anatexis and metamorphism in the Ograzhdenian supercomplex. For to verify this hypothesis, new detailed structural and isotopic studies are needed.

Key words: Serbo-Macedonian Massif; Ograzhden Unit; Frolosh Greenstone Belt; Rhodope Massif;
Late Proterozoic and Palaeozoic tectonics

1. INTRODUCTION:

The Morava-Rhodope Alpine Collage (MRAC) and the Serbo-Macedonian Massif (SMM)

The Alpine tectonic structure of the Balkan Peninsula is dominated by the Vardar Suture. This relict from the Mesozoic Tethyan Vardar Ocean divides the Peninsula in two well-outlined domains: the western belt of Hellenides-Albanides-Dinarides of Tethyan character, and the eastern belt of the Balkanides *s.l.* characterized by a PeriTethyan Mesozoic evolution. Outwards from the Vardar Suture, and along a transect trending North-

East towards the Moesian Platform, three major belts may be distinguished (e.g., Dabovski et al., 2002; Zagorchev et al., eds., 2009) in the Late Cretaceous structure: the “internal” Morava-Rhodope Zone, the Late Cretaceous Srednogorie Volcanic Arc transformed by end-Cretaceous time into the Srednogorie Orogen, and the Balkanide Orogen that consists of the Stara-planina (Balkan) Zone, the Transitional Zone and the Fore-Balkan Zone.

Whereas the south-western parts of the Morava-Rhodope Zone possess a south-western vergence being subducted by the Vardar slab, the north-eastern parts are thrust to North-East over the Srednogorie, and each of the following external zones has the same northern to north-eastern vergence towards and over the Moesian Platform. Older tectonic ideas regarded the structure of the Peninsula as consisting of two divergent orogenic belts (southern Dinaridic and northern Balkanidic “branches of the Alpine orogen”) divided by a median Rhodope Mass (*sensu* Cvijić), median belt (in the sense of J. Brun) or a Zentralmassif (*sensu* Kossmat).

The Morava-Rhodope, Srednogorie and Stara Planina zones are characterized by a pre-Alpine basement and a Mesozoic and Cenozoic cover. The basement derived from pre-Hercynian continental and oceanic crust and Hercynian continental crust. The cover consists mostly of sedimentary formations of peri-Tethyan affinity, i.e., formed in epi-continent shallow seas and back-arc environments. The Triassic volcanic activity is related to rifting in the Moesian Platform and along the Maritsa fault belt (at the boundary between the Morava-Rhodope and the Srednogorie). Amagmatic deeper sedimentation environments are related to troughs with restricted occurrences: the East-Balkan (Kotel) trough (continuous Triassic to

Middle Jurassic sequence with olistostromes; Mid-Jurassic folding), the Jurassic Treklyano trough, and the Late Jurassic – Early Cretaceous Nish-Troyan trough. Extensive igneous activity is typical of the Late Cretaceous Srednogorie Zone which developed from an epicontinental rift with crustal thinning to a volcanic arc with deeper sedimentary basin environment.

Basement and cover tectonic elements have been extensively deformed and imbricated throughout the Alpine orogenesis. Alpine deformations have been superimposed over the pre-Alpine basement elements at different structural levels, and correspondingly, in different P-T metamorphic conditions.

The Morava-Rhodope Zone has a highly heterogeneous structure. It consists of structural elements of different ages and provenance that have been gathered in a specific collage. From west to east, i.e., from the Vardar Suture towards the Srednogorie Zone, the following major structural elements have been distinguished: eastern marginal strip of the Vardar Zone that passes to south-east into the Circum-Rhodope Belt; Serbo-Macedonian Massif (partially identified as Morava Zone s.l.); Morava Zone s.s. (Palaeozoic units thrusted mostly in mid-Cretaceous times over the Struma Zone); Struma Zone; units of the Rhodope Massif.

2. FROLOSH GREENSTONE BELT (FGB)

The Frolosh Greenstone Belt is traced directly at a distance of about 200 km between the Belasitsa Horst at the South (on the territory of Macedonia) and the area of Trun to the North (Fig. 1). It is widely accepted that before the Alpine tectonics the belt had been connected with the large outcrops of similar composition that are traced between Shipka Stara planina Mountain and the Deli Jovan and Iuți massifs in West Stara planina and the South Carpathian Mountains, respectively (e.g., Haydoutov, 1989; Haydutov et al. 2012). The possible correlations and geodynamic considerations shall be discussed in the final parts of the present paper.

The principal constituents of the FGB are the Frolosh metamorphic complex (FMC) and the Struma diorite complex (“formation”, SDC). Known since the pioneer works in the 19th century, their first detailed description dates from the first half of the 20th century when Stefanov and Dimitrov (1936) coined the name Struma diorite forma-

tion. There is a close relation between this Struma diorite complex, and the greenschist-facies rocks of the Frolosh complex: the Struma diorites to granites occur solely amongst the rocks of the latter exhibiting different kinds of contacts, – from irregular transitional contacts to sharp intrusive ones (Zagorčev, 1966, 1987; Zagorchev, 2001).

The Frolosh metamorphic complex (FMC) consists (Zagorčev, 1987) mostly of greenstones: metadiabases, metamorphosed tuffs, actinolite- and chlorite-actinolite schists. Phyllites (sericite-chlorite schists), albitophyres to keratophyres, calcareous schists to impure marbles, and metapsammites (metasandstones to fine-pebble metaconglomerates) have been also found. A few bodies of serpentized ultramafics have been observed mostly as tectonic lenses: a body of lherzolite within the green schists east of the village of Frolosh (Despov, 1959; Zagorčev, 1966), and a thin (5 – 8 m) lenticular slice of peridotite from the basement tectonically inserted along the Garbino thrust parallel

to the schistosity within the basal parts of the Lower Triassic section that covers the Frolosh

basement near the village of Garbino (Zagorčev, 1985; Zagorčev, 2001; Graf, 2001).

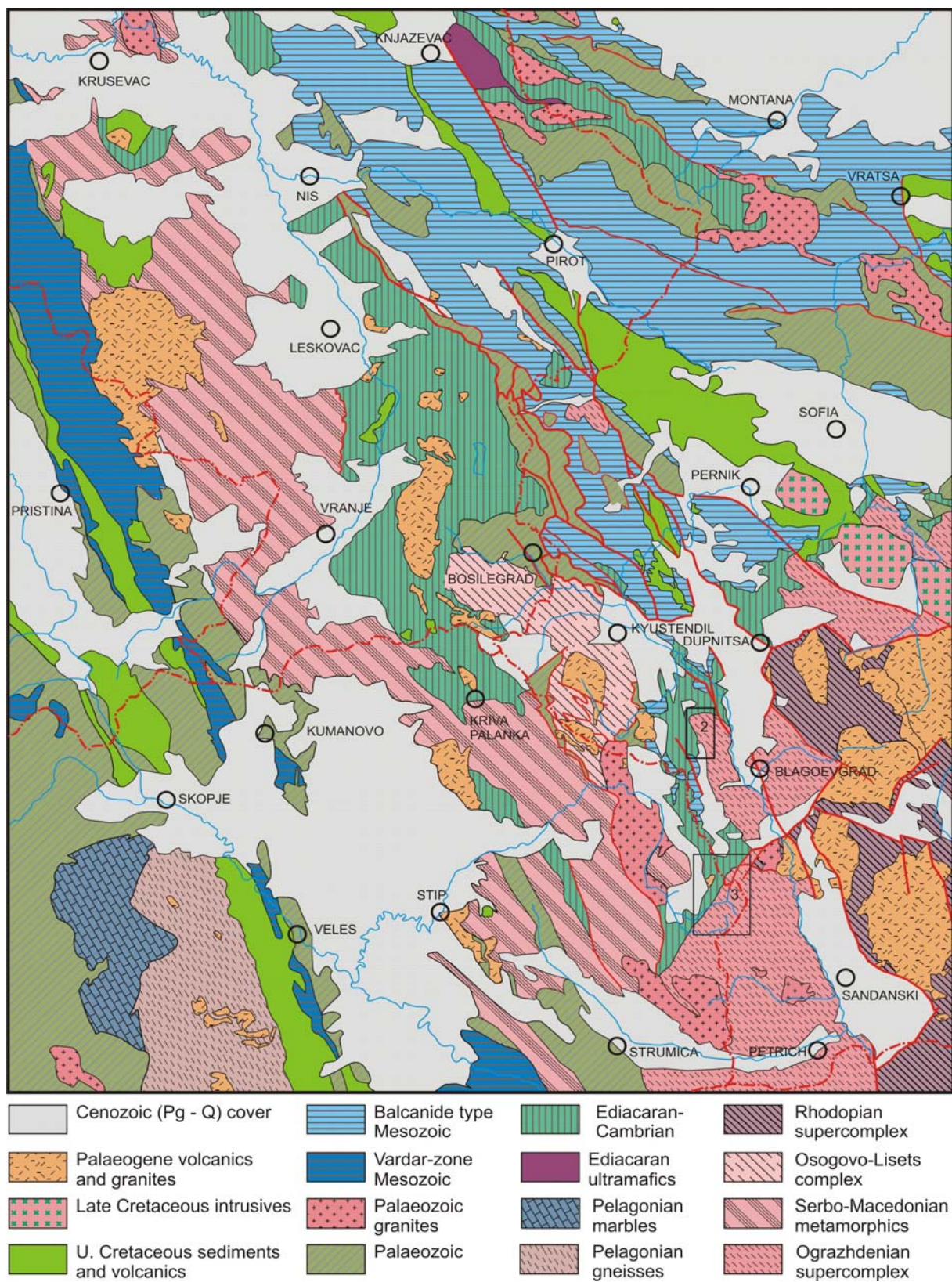


Fig. 1. Simplified geological map for the position of the Frolosh Greenstone Belt and the Ograzhdenian metamorphic supercomplex in the Alpine orogenic structure of the Balkan Peninsula. The detailed map areas (Figs. 2 and 3) are indicated.

A number of metabasic bodies have been reported by Zagorčev (1966), and Haydoutov et al. (1993) interpreted them as two large blocks of metabasites that belonged to oceanic crustal fragments. Zagorčev (1966) pointed at the presence of 3 age groups of basic rocks: ultramafic and mafic bodies pre-dating the greenschist-facies metamorphism, ultramafics and mafics that represent a (mostly) early phase of the Struma diorite formation, and a late phase of microdiorite, dolerite and lamprophyre dykes.

The petrologic features of the Frolosh metamorphic complex (Frolosh Formation) are important both for reconstruction of the protoliths, and for understanding their tectonometamorphic evolution. In some cases, the tectonic reworking of the rock has been so extensive that the exact nature of the protolith cannot be established, and the rock is designated simply as “greenstone” or “green schist”. The dominant actinolite schists and chlorite-actinolite schists are usually of lepidoblastic, lepidogranoblastic or nematoblastic texture, the melanocratic strips being built of actinolite, chlorite, epidote, sphene, magnetite, and the leucocratic ones, of quartz and albite with minor amounts of epidote and chlorite. Actinolite and quartz form occasional glomeroblastic isometric intergrowths with signs of rotation. Relicts of ophitic texture are present, too, with rotation and replacement of the primary plagioclase by epidote-albite-quartz aggregations. Relicts of the primary minerals and blastoophitic texture are better preserved in the granular metadiabases: primary relatively coarse (1–2 mm) plagioclase and hornblende (probably also pyroxene) hypidiomorphic crystals totally replaced by albite-quartz-epidote and chlorite-actinolite aggregates, respectively. The intensive deformations have only slightly affected the central parts of some of the massive metadiabase bodies as well as the rarely preserved pillows. The latter are built of glomeroblastic aggregates of actinolite, quartz, albite, epidote and abundant chlorite, with huge grains or skeletal shapes of magnetite. Some of the metadiabase bodies pass gradually into metagabbrodiabases and metagabbroic rocks.

Metakeratophyres and acid metatuffs have a banded structure and granoblastic to lepidogranoblastic texture. They are usually built of fine- to microgranular aggregates of allothriomorphic quartz, albite and epidote with single large crystals of mafic mineral entirely replaced by glomeroblastic epidote aggregates. Coarse single plagioclase

and quartz crystals are also entirely replaced, by glomeroblastic quartz-albite aggregates. Usually these rocks are strongly deformed into a thin millimetric alternation of quartz and albite bands.

Phyllites often interlayer with actinolite-chlorite schists, or rarely (along the road towards the former barracks near Kadiytsa Peak; stratotype of the Frolosh Formation) with thin beds of calcareous schists and impure marbles. The thickness of the thin beds in the calcareous schists varies between 1 and 10 mm. Light bands consist of granoblastic quartz-calcite aggregates, some bands being enriched in epidote and sphene. The melanocratic bands are finer-grained, with lepidoblastic structure, and are built of chlorite, epidote and magnetite with some andesine fine crystals, and rare larger calcite crystals.

Metapsammites have been recorded along the road from the Kopriven River towards Frolosh (Figs. 2, 3) and near the bridge on the Pehčevo-Berovo road in Macedonia (Stojanov et al. 1997). Another more controversial locality (Gabrovdol) has been described by P. Gochev (s. Tenchov, Zagorčev, 1989) but later Bonev (1996; Bonev et al., 1995) denied their metapsammitic character. A revision of all metapsammitic localities with a detailed mapping and provenance analysis is needed, and detrital zircon datings can be most helpful. The metapsammites observed are small- to medium-grained (0.5 to 2 – 3 mm rounded grains) with a basal fine-grained recrystallized groundmass of sericite and chlorite with some epidote, quartz and albite-oligoclase. The grains are mainly of quartz and feldspar, some fine (2 – 5 mm) rounded pebbles of granitoid composition being also present. The composition of the metapsammites suggests a close to moderately distant source with continental character although more detailed research is needed for to prove this assumption.

The Struma diorite complex (introduced as Struma diorite formation) consists of a wide range of basic to acid igneous rocks. The most frequent rock varieties are diorites to quartzdiorites with basic (mostly gabbro) enclaves. Gabbroic rocks are observed also as separate bodies or parts of the diorite bodies, and in a few cases (e.g., the Padarnitsa Hill north of Boboshevo) such bodies contain pyroxenite parts probably formed as cumulates. Plagiogranites and granites occur either as separate bodies and dykes that often intersect the bigger diorite bodies, or develop as anastomosing dykes with transitional contacts with the host diorite.

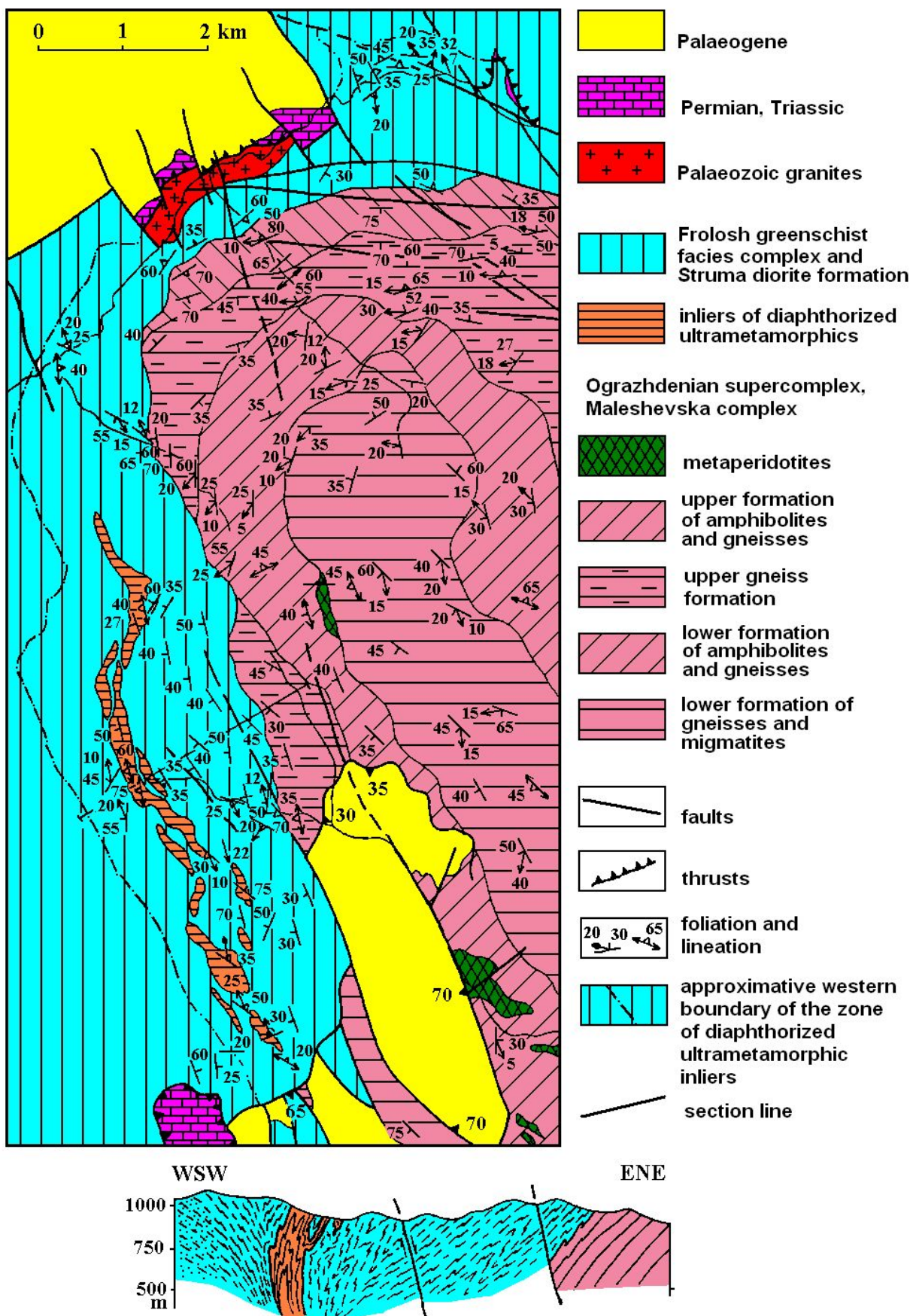


Fig. 2. Geological map of the Frolosh part of the Frolosh Greenstone Belt (after Zagorčev, 1974, Fig. 1)

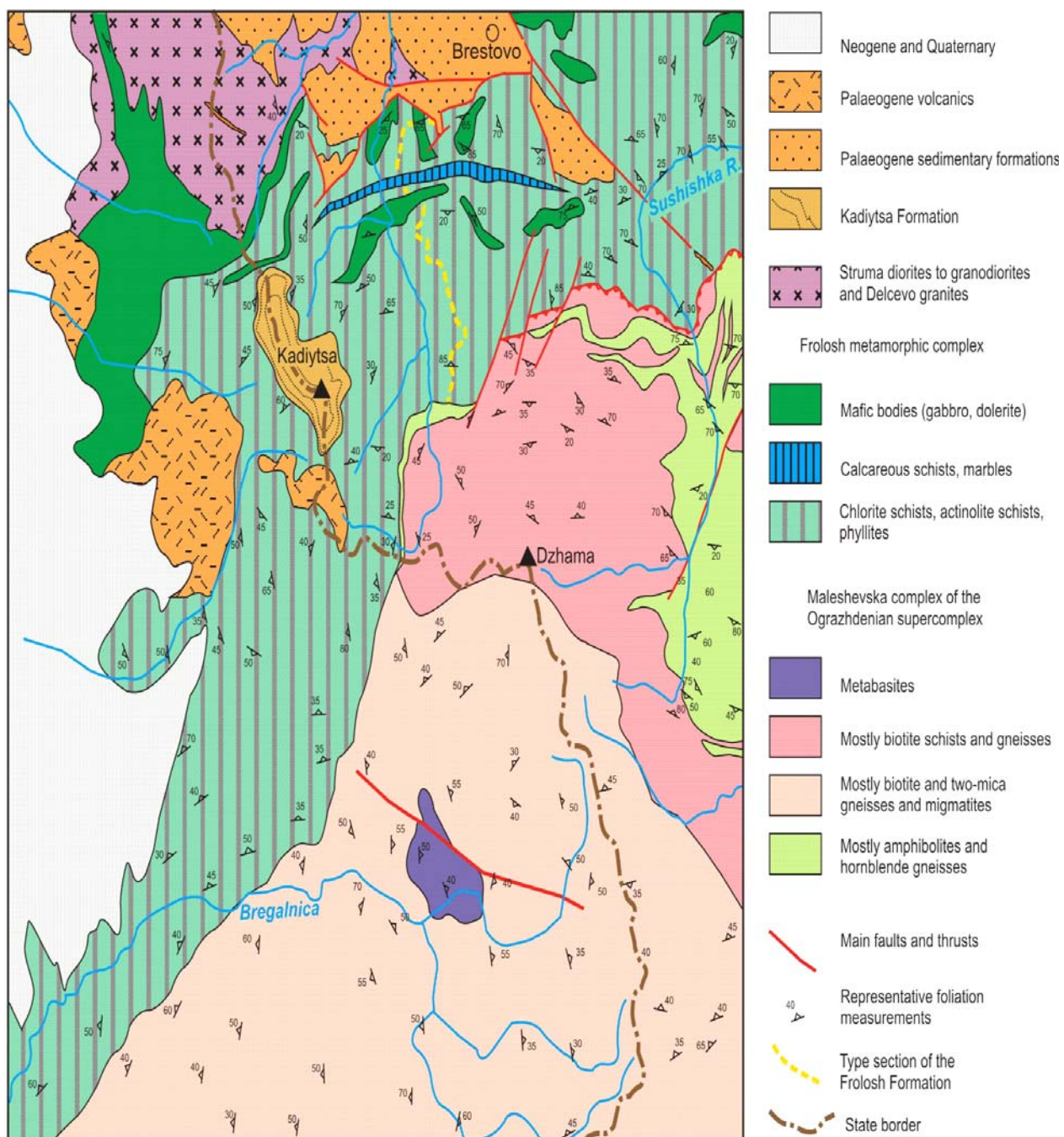


Fig. 3. Geological map of the Kadiytsa part of the Frolosh Greenstone Belt
(after Zagorčev, 1989; Stojanov et al., 1997; Milovanov et al., 2008)

The character of the contacts of the diorite bodies with the green schists and rocks of the Frolosh complex shows also a wide variety: either sharp intrusive contacts, or uneven transitional contacts with gradual feldspathization and development of patches and bands of diorites within the Frolosh green rocks (Fig. 4).

The last igneous phase is usually represented by basic dykes of dolerites, microdiorites and lamprophyres. Outcrop observations usually reveal

that the basic dykes either cross-cut all rock varieties, late granites included, or some late granite dykes intersect the basic rocks. However, observations in the road cuttings south of Delčeve (Stojanov et al., 1997) suggest the presence of more complicated relations: thick basic dykes cross-cut the diorites but locally are boudinaged and partially melted within the latter suggesting mixing and mingling of basic and acid magmas.



Fig. 4. Field photographs of outcrops of the Frolosh complex and the Struma diorite formation:

a – metadolerites, metatuffs, metasandstones; outcrop in the road cuttings south of Frolosh; **b** – another outcrop along the same road; **c** – isoclinal folds in phyllites and metatuffs, detail of a; **d** – metasandstones, detail of a; **e** – Struma diorites in the Skrino Gorge (outcrop in road cuttings near Pastuh); **f** – dioritization in metadolerites, and late anastomosing epidote veins (near the contact between the metadolerites and the Struma diorite, at the western entrance of Pastuh); **g** – basic enclave in diorite (same outcrop); **h** – Struma diorite with enclaves and with cross-cutting basic dyke (almost horizontal) displaced by fault (same outcrop).

Photos a, c, e, f and g taken by D. Milovanović, b, d and h – by I. Zagorchev

The chemical composition of the rocks of the Frolosh Greenstone Belt shows large variations of the main components (Fig. 5). The basic rocks (no discrimination between earlier basic rocks and the basic rocks related to the Struma diorites has been made in the references used) shows a remarkably good arrangement of the figurative points in the magnesian gabbros field, and according to Haydoutov et al. (1992, 2012) corresponds well to

MORB chemistry although close to the Ca-alkaline field. Haydoutov et al. (2012 and former publications) made a thorough analysis of the chemistry (including REE distribution), and regard these rocks as typical MORB ophiolites but mark that the so-called parallel dykes are situated in the field of E-MORB on the Wood's (1980) diagram which is also typical of the intraplate tholeiitic basalts and their differentiates.

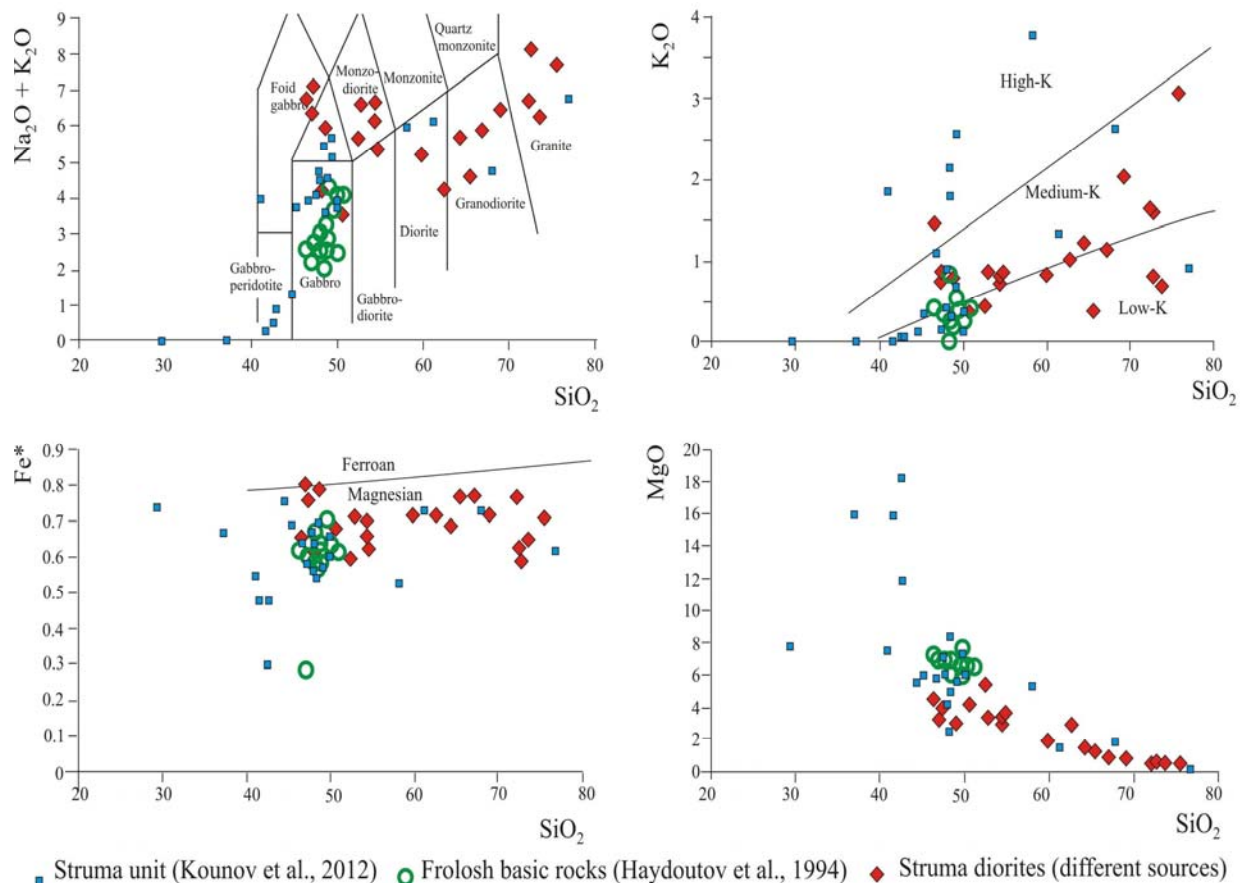


Fig. 5. Diagrams for the chemical composition of the rocks of the Frolosh Greenstone Belt.
 Primary data after Haydoutov et al. (1992, 1993, 1994), Graf (2001), Kounov (2002) and Kounov et al. (2012).

The data of Kounov (2002, Kounov et al., 2012) show by far a greater dispersion of the samples: from peridotites to gabbros and alkaline gabbros. Even a greater dispersion is observed on the $\text{K}_2\text{O}-\text{SiO}_2$ diagram, the potassium content varying from very low-K to extremely high-K even in rocks of gabbroic composition. These features allow for different interpretations such as: (i) a great diversity of the initial magmas, (ii) magma mixing and mingling, and (iii) alkali and silicic metasomatism at different stages of the rock evolution. The composition of the Struma diorite complex varies from gabbro and alkaline gabbro through diorite,

monzodiorite and granodiorite to granite, and again, with a considerable variability in the alkali, potassium and iron content, and a more consistent smooth evolution of the magnesium content. Haydoutov et al. (2012) specially indicate at the Ca-alkaline character of the Struma diorite complex, and their pronounced higher alkalinity when compared to the Berkovitsa island arc association from the Stara planina belt. They also have pointed (Haydoutov et al., 1992, 2012) at the very different chemistry of the metaplagiogranites from the Kopriven area which in turn also indicates a different magmatic source.

The U-Pb zircon dating (Graf, 2001; Kounov, 2002; Zagorchev et al., 2011a,b, 2012; Kounov et al., 2012; Kiselinov et al., 2014; Antić et al., 2015) yielded Cadomian (Ediacaran – Cambrian) ages (Table 1), mostly within the time span 578 – 514 Ma (Figs. 6 and 7). Taking into account the full range of the zircon dates (within the confidence limits), the data are partitioned as follows (from geologically the oldest to the youngest rocks):

(1) Metadolerites of the Frolosh metamorphic complex: between 517.1 ± 2.1 and 532.1 ± 1.5 Ma.

(2) Basic rocks (gabbros, in enclaves inclusive): between 552.3 ± 1.3 and 578.6 ± 1.8 Ma.

(3) Diorites and quartz-diorites: between 514.8 ± 1.6 and 569 ± 11 Ma.

(4) Granites: between 536 ± 7 (Delchevo), 543.5 ± 3.9 (Rakovo) and 549.6 ± 1.8 – 560.5 ± 5.1 Ma (near Tsurvishte).

(5) Detrital zircons in the covering Kadiytsa Formation: 518.7 – 520.9 Ma.

The analysis of all single zircon measurements from the samples from the four main rock varieties of the Frolosh complex (Fig. 8) shows practically the same distribution pattern for the oldest varieties: metadolerite, gabbro from enclave and diorite. This pattern corresponds to latest Ediacaran (from around 555 Ma) to latest Cambrian (c. 500 Ma). Most unexpectedly, the youngest rocks (K-feldspar granite veins with diffuse boundaries within the diorite at Tsurvishte) yield a distinctive pattern with strictly Ediacaran ages: from c. 575

Ma to 540 Ma. For the time being, we are not able to give a logical explanation to this anomalous fact: the geologically youngest rocks yield the oldest age. All rocks of the Frolosh metamorphic complex and the Struma diorite formation have been formed within a relatively restricted time span (late Ediacaran to Cambrian), and these data confirm the ideas about the Cadomian origin of the Frolosh Greenstone Belt.

In the Bulgarian geological literature the opinion about the Ediacaran-Cambrian (Vendian-Cambrian) age of the FMC and SDF has been dominant for nearly a century (s. e.g., Zagorčev, 1966, 1987; Aleksić et al., 1988, and references therein). S. Dimitrov (1939) suggested a Devonian age for the Diabase-phyllitoid formation, and this idea has been supported by Vrablianski et al. (1962) and some other authors for the Stara-planina region. These ideas were rooted in the restricted knowledge about the corresponding rock complexes, and the attribution of all greenschist-facies (and even lower-grade) rocks to the *Diabase-phyllitoid formation*. With the discovery of the Devonian System in Bulgaria (Spassov, 1960) and the consecutive age differentiation of the greenschist-facies rocks, the pre-Ordovician age of the FMC, SDF and their correlates has been gradually confirmed with sufficient geological evidence. The Devonian in SW Bulgaria has been thoroughly studied (Spassov, 1973).

Table 1

U-Pb Concordia zircon data for the rocks of the Frolosh metamorphic complex, Struma diorite complex and the Kadiytsa formation

Sample	Rock variety	Locality	Age range, Ma	Source
294	metadolerite	Near Tsurvishte	517.1 ± 2.1 – 532.1 ± 1.5	Zagorchev et al. 2011
529	metadolerite	Sushitsa	521.7 ± 6.9	Kiselinov et al. 2014
K928	gabbro	Near Razhdavitsa	557 ± 3.5	Graf 2001*; Kounov et al. 2012
295BF	basic enclave	Near Tsurvishte	552.3 ± 1.3 – 578.6 ± 1.8	Zagorchev et al. 2011
	Struma diorite	Struma Unit	569 ± 11	Kounov* 2002
AK229	Struma diorite	Struma Unit	560.1 ± 8.5	Kounov et al. 2012
295	Struma diorite	Near Tsurvishte	514.8 ± 1.6 – 531.4 ± 4.2	Zagorchev et al. 2011
296	KFs granite	Near Tsurvishte	549.6 ± 1.8 – 560.5 ± 5.1	Zagorchev et al. 2011
	Granite	Delchevo	536 ± 7	Antić et al. 2014
	Granite	Rakovo	543.5 ± 3.9	Milovanov et al. 2009
531,532	Sandstone, Kadiytsa Fm.	Kadiytsa Peak	518.7 – 520.9 (detrital grains)	Kiselinov et al. 2014

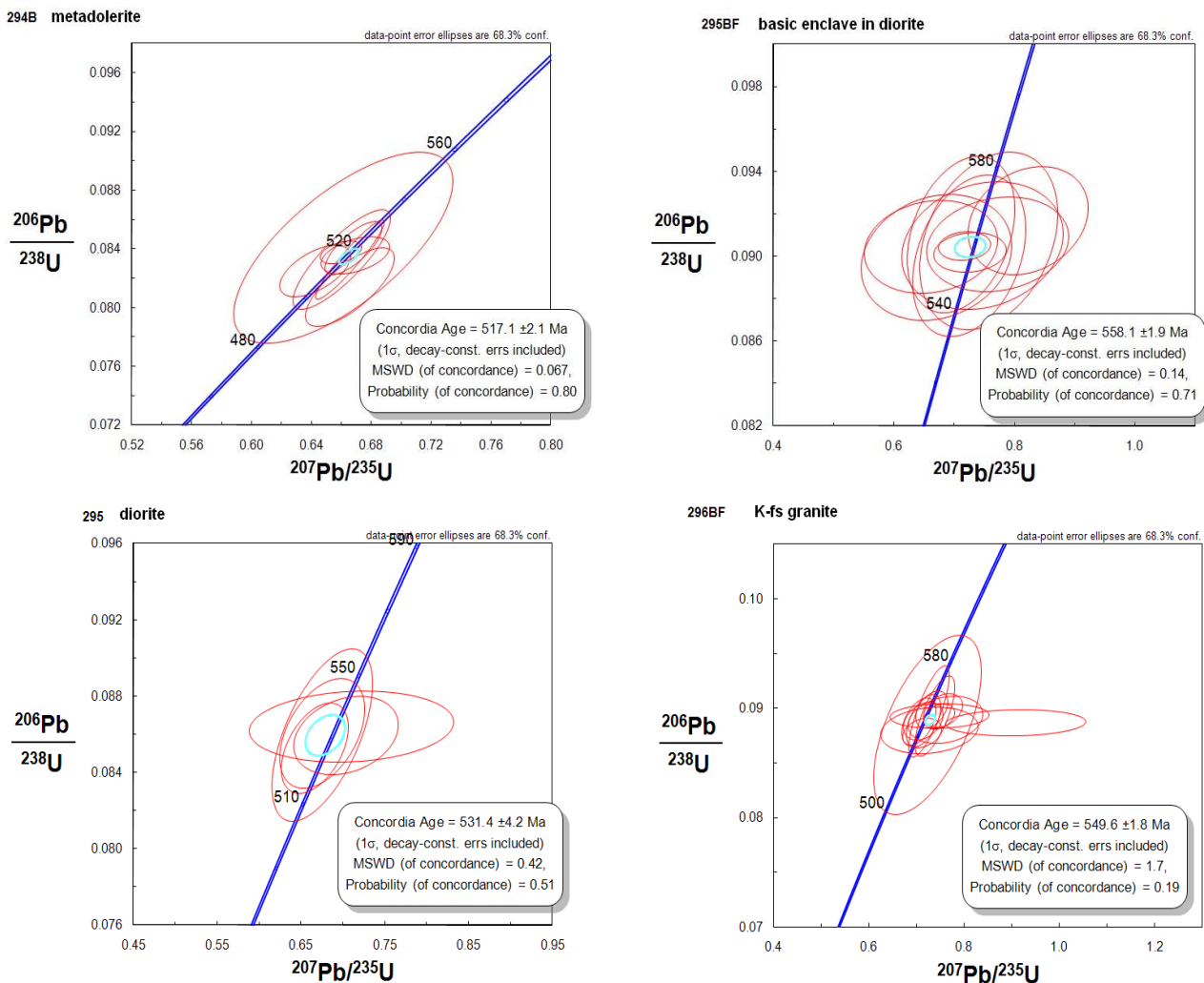


Fig. 6. Concordia diagram for the zircons from the Frolosh Greenstone Belt

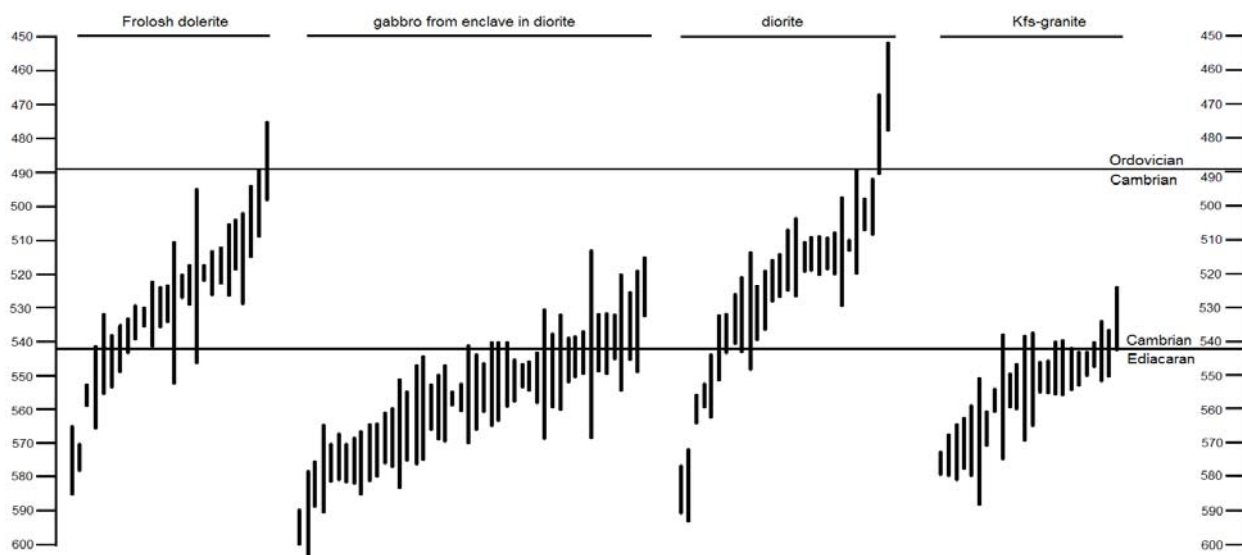


Fig. 7. Diagram for the apparent ages of zircons from the Frolosh Greenstone Belt



Fig. 8. Field photographs of outcrops of the Maleshevska complex of the Ograzhdenian supercomplex in the Ograzhden unit: **a** – augen gneisses and stromatic migmatites in the road cuttings along the road from Mikrevo to Tsaparevo; **b** – norite with aplitoid veins in the village of Gorna Ribnitsa; **c** – biotite gneisses with layer of quartzo-feldspathic gneisses, all subject of migmatization (road cuttings near the tunnel south of Yavorov Railway Station; near sample 302); **d** and **e** – tourmaline pegmatite transformed in quartzo-feldspathic gneiss hosted in tourmaline-biotite schists (along the road from Mikrevo towards Tsaparevo, second turn above Mikrevo); **f** – outcrop of metagranite (site of sample 307) along the road between the villages of Ribnik and Lebnitsa; **g**, **h** and **i** – details of same outcrop showing different degree of resorption of xenoliths from biotite schists and biotite migmatites.

Photographs by I. Zagorchev

Moreover, basic (diabase) magmatism has been proven also in younger Palaeozoic formations structurally and stratigraphically distinctive from the Cadomian sequence: in the Ordovician(?) Bazovitsa formation and the Lower Devonian in the Kraishte area (Zagorčev, Bončeva, 1988; Zagorčev, 2001), the latest Silurian? – Devonian Razhcha Formation in the Osogovo Mt. (Lakova et al., 1995; Lakova, 1997; Stojanov et al., 1997), and the still undated Kadiytsa Formation (Zagorčev, 1987) around the Kadiytsa Peak (Fig. 3) at the Bulgarian-Macedonian border.

Bonev et al. (1995) and Ricou et al. (1998) arbitrarily correlated the FMC with very low-grade formations of Jurassic age, and based on this erroneous supposition made far-fetched conclusions about the Vardar-Rhodope relations. However, besides the geological evidence (Zagorčev, 2000), the groundless ideas about a Jurassic age of the FMC have been rejected also based on U-Pb zircon isotopic studies (Graf, 2001; Kounov, 2002; Zagorčev et al., 2011a,b; Kounov et al., 2012).

3. OGRAZHDENIAN SUPERCOMPLEX

The Ograzhdennian supercomplex has been introduced for amphibolite-facies metamorphic rocks that crop out in the mountains Vlahina, Maleshevska, Ograzhdenn and Belasitsa in the territories of SW Bulgaria and Macedonia (s. Zagorčev, 1996, 2001, and references therein). Two units (lower, Troskovo Amphibolitic Group with three formations, and upper, Maleshevska Gneiss-Migmatitic Group) have been introduced as formal lithostratigraphic units but the complex internal folded and sheared synmetamorphic structure does not allow for a reliable lithostratigraphic description, and these two units are now regarded as informal metamorphic complexes (from bottom to top in the geometric generalized section): Troskovo amphibolitic complex and Maleshevska gneiss-migmatitic complex. The position and character of a third (Belasitsa) complex regarded as situated at the base of the section are not clear because of even greater tectonic difficulties, and it is possible that it represented a part of the Maleshevska complex situated in the inverted limb of a huge recumbent fold. Both complexes are exposed in the cores of two major tectonic units within the Alpine Morava-Rhodope tectonic zone: the Lisiya core of the Struma unit, and the Ograzhdenn unit.

The Troskovo amphibolitic complex crops out mostly in the southern part of the Lisiya crystalline core (in southern Vlahina Mountain) of the Struma unit, and has a limited occurrence in the southwesternmost part of the Maleshevska Mountain (on Bulgarian territory, north-east of the Zlatarevo checkpoint at the border with Macedonia). Three lithostratigraphic units have been introduced (Zagorčev, 1989a) as follows (from bottom to top): Dokatichevo Formation (dominant amphibolites and biotite amphibolites interlayered

with biotite-hornblende gneisses and biotite quartzo-feldspathic gneisses; relict lensoid bodies of massive garnet amphibolites, and rarely of metaperidotites); Starirechka Formation (biotite and two-mica gneisses and schists interlayered with hornblende-biotite gneisses and amphibolites; thin amphibolite dykes; few lensoid bodies of metaperidotites); Chetirka Formation (amphibolites, massive garnet amphibolites, zoisite-hornblende gneisses, biotite-garnet-hornblende gneisses, quartzo-feldspathic gneisses; few lenses of gabbro-amphibolites; several lensoid 3–70 cm thick marble layers). The composition of the Troskovo complex points at metavolcanic protoliths with some metasedimentary interlayers, the thickest ones (total thickness of 400 – 500 m) being concentrated in the Starirechka Formation. The rocks of the Troskovo complex build the large Simitli reclined fold (Zagorčev, 1976b), its core being outlined also by the outcrops of the Starirechka Formation.

The Maleshevska gneiss-migmatitic complex builds the northern part of the Vlahina Mountain and almost entirely, the mountains Maleshevska and Ograzhdenn (Ograzhdenn Unit). It consists of predominant biotite and two-mica gneisses, often rich in mica and in transition to biotite schists. They are occasionally garnet- and graphite-bearing. Quartzo-feldspathic gneisses are frequent in relatively thin layers. In the Ograzhdenn Unit, tourmaline-biotite schists, staurolite-kyanite and sillimanite-bearing biotite schists are present, too. Amphibolites are widespread, mostly as layers traced at distances of several kilometers, and often boudinaged, too. Irregularly shaped or lensoid amphibolite bodies are also present as well occasional lenses of metaperidotites, metapyroxenites and

metamafics (gabbro, norite to troctolite). The rocks of the Maleshevska complex are irregularly, and often extensively migmatized, with formation of different migmatite types (s. Zagorchev, 1996): stromatic, diktyonitic, agmatic, porphyroblastic, nebulitic, etc. They are intruded by several generations of granitoids. The oldest granitoids (Zagorčev, 1976a; Zagorchev, 1996) are diatexitic quartz-diorites, granodiorites and granites that contain abundant xenoliths (formerly skialiths) of biotite schists, biotite and two-mica gneisses and migmatites, amphibolites, pegmatites, and even, ellipsoidal quartz xenoliths sometimes arranged in a bead-like manner hinting at former disrupted quartz veins. A body of similar (meta)granitoids (Ribnik granitoids) has been dated by the U-Pb method on zircons as Ordovician (Table 2, Figs. 9, 10, 12). Later granitoids (mostly granodiorite and granite) are coarse-grained to porphyric, massive, and have been dated (Table 2) as Early to Middle Triassic.

The structure of the Maleshevska complex differs in the Lisiya core (Vlahina Mountain) and in the Ograzhden unit. In the Lisiya core, the Maleshevska complex is situated over the Troskovo amphibolitic complex and is covered by the Frolosh complex. The layers of the Maleshevska complex are strongly elongated in NNW-SSE direction, and are paralleled by fold axes and mineral lineations. They outline a single (Lisiya) anticline situated unconformably over the Troskovo complex of the Simitli reclined fold (s. Zagorčev, 1981). In the Ograzhden Unit, a strongly compressed and also NNW-SSE elongated isoclinal structure of subparallel SW-vergent synclines and anticlines with extensive shear in the limbs is overprinted over a complex structure with interference pattern of WNW-ENE, NE-SW and NNW-SSE trends (Zagorchev, 1996).

Numerous field and laboratory data point at a complex polymetamorphic and polydeformational evolution of the Ograzhdenian supercomplex and its structures (s. Zagorčev, 1976a; Aleksić et al., 1988; Zagorchev, 1996, 2001). The overall metamorphic conditions correspond to the amphibolite facies. Zidarov, Nenova (1996, 1999) and Nenova, Zidarov (2008) reported relicts of eclogite-facies mineral associations in the metabasic bodies at Gega and Gorna Ribnitsa villages. The polymetamorphic character of the Ograzhdenian supercomplex is reflected also in the results of the numerous but still insufficient isotoping datings of different rock varieties. The full results of our own datings

are shown in Annexes 1–8 and Figs 7 and 8., and the synopsis of all published data is shown in Figs. 11 and 12.

The oldest zircon data come from the metabasic rocks (partially amphibolitized gabbro-norite) in the vicinity of Gorna Ribnitsa village (Zagorchev et al., 2014). Numerous zircon data points are scattered between c. 2600 and 1125 Ma suggesting an upper intercept of about 2.7 Ga, and a lower one, at c. 1.0 Ga. Different interpretations may be made but they certainly point at the presence of very old (Neoarchean) recycled material. The majority of the data points are situated over the Concordia or near it, and cover the interval between 877.5 and 503.0 Ma. They may correspond to a Neoproterozoic protolith with culminating Ediacaran-Cambrian (Cadomian) emplacement and cooling. Such a conclusion is consistent also with the Rb-Sr whole rock isochrone obtained on 10 whole-rock samples from different rock varieties of the Maleshevska complex in the Tsaparevo area (Lilov et al., 1983) confirmed also on four additional samples analyzed by S. Moorbat at the University of Oxford (Table 2). Zidarov et al. (2007) reported zircons from a metagranite at Kolarovo (Belasitsa Mountain, Ograzhden Unit) with core dates between c. 750 and 555 Ma, and outer rims dated at c. 520 Ma. Zircons dated between 600 and 550 Ma are also present in the Ribnik metagranite (Fig. 10, Annex 5, Table 2). All these data point at a Cadomian history of the supercomplex which has been heavily overprinted by a later stage of very extensive metamorphism and anatexis in Ordovician and Silurian times as supported by the numerous ages obtained for zircons from gneisses, migmatites and metagranites (mostly diatexitic) within the range latest Cambrian – Late Silurian (c. 490 – 420 Ma, Figs. 9, 10, 12). An interesting result of the U-Pb zircon studies is the presence of Cadomian relict zircons in the Ribnik metagranitoids, and the U-Pb Concordia zircon ages in them that are older than the Concordia zircon ages of the geologically older host migmatites. These facts clearly indicate that the eutectoid leucosome of the host migmatites has been mobilized for a longer period of time (compared to the “encapsulated” granitoid body), and namely, up to Late Silurian times.

The youngest thermotectonic event is related to the intrusion of the Permo-Triassic granites that could also have some effect (with zircon crystallization) in their immediate vicinity.

Table 2

U-Pb Concordia zircon data for the rocks of the Ograzhdenian supercomplex

Sample	Rock variety	Locality	Age range, Ma	Source
WR	isochron	Maleshevska Mt.	Rb-Sr $531 \pm 13 - 548 \pm 30$	Lilov et al. 1983; Zagorchev et al. 1989
	Metagranite (zircons)	Kolarovo, Belasitsa Mt	518 ± 19 (outer rims) $750 \pm 2.5 - 555 \pm 10$ (cores)	Zidarov et al. 2007
302RW	Bi migmatite	Yavorov RW Stat.	$456.3 \pm 1.8 - 475.1 \pm 2.6$	Zagorchev et al. 2011,2012
GR2	Amphibolite after norite	G. Ribnitsa	452.8 ± 2.2	Zagorchev et al. 2011,2012
304	Bi gneiss	Near Mikrevo	$439.4 \pm 1.6 - 451.8 \pm 1.5$	Zagorchev et al. 2011,2012
306	Augengneiss	Ribnik	$433.0 \pm 1.5 - 445.4 \pm 1.3$	Zagorchev et al. 2011,2012
AK228	Two-mica orthogneiss	Ograzhden	476 ± 6	Kounov et al. 2012
	leucosome	Ograzhden	461 ± 18	Zidarov et al. 2007
	Plagiogneiss	Maleshevska Mt.	472 ± 4	Antić et al. 2014
	metagranite	Lozen	451.9 ± 1.3	Macheva et al. 2006
307	metagranite	Ribnik	461.2 ± 2.0	Zagorchev et al. 2011,2012
	granite	Igralishte	243.28 ± 0.84	Peytcheva et al. 2009
	granite	Skrut, Belasitsa	248.85 ± 0.70	Zidarov et al. 2007

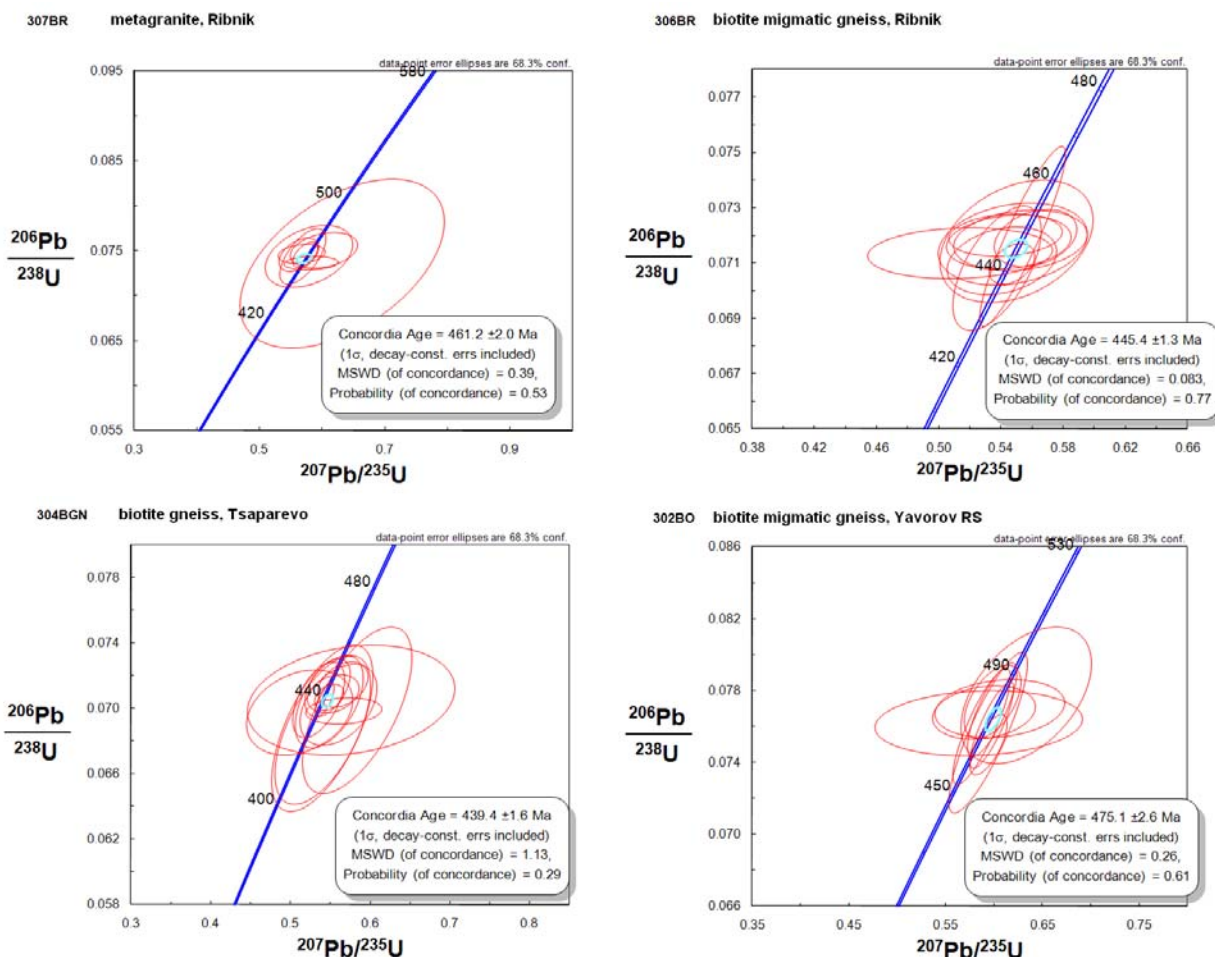


Fig. 9. Concordia diagram for the zircons from the Ograzhdenian supercomplex

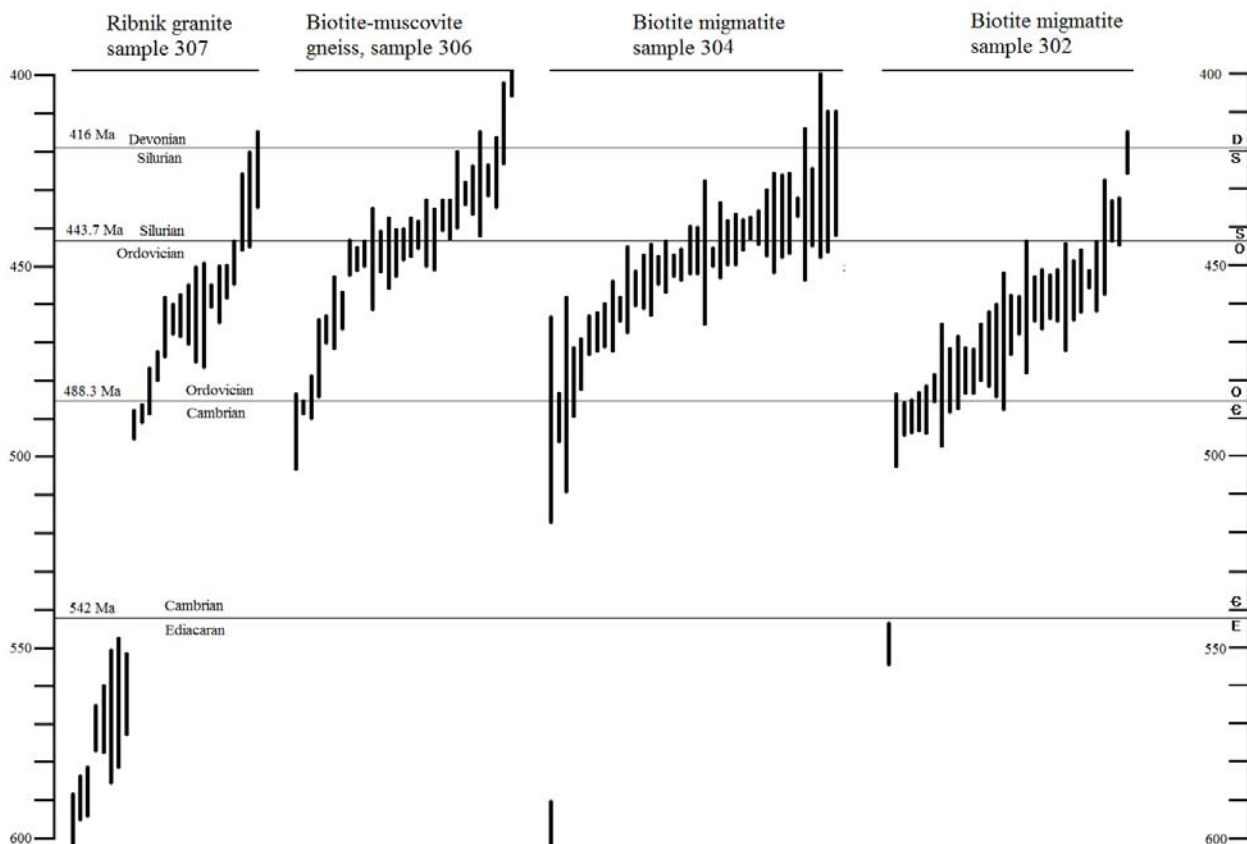


Fig. 10. Diagram for the apparent ages of zircons from the Ograzhdennian supercomplex

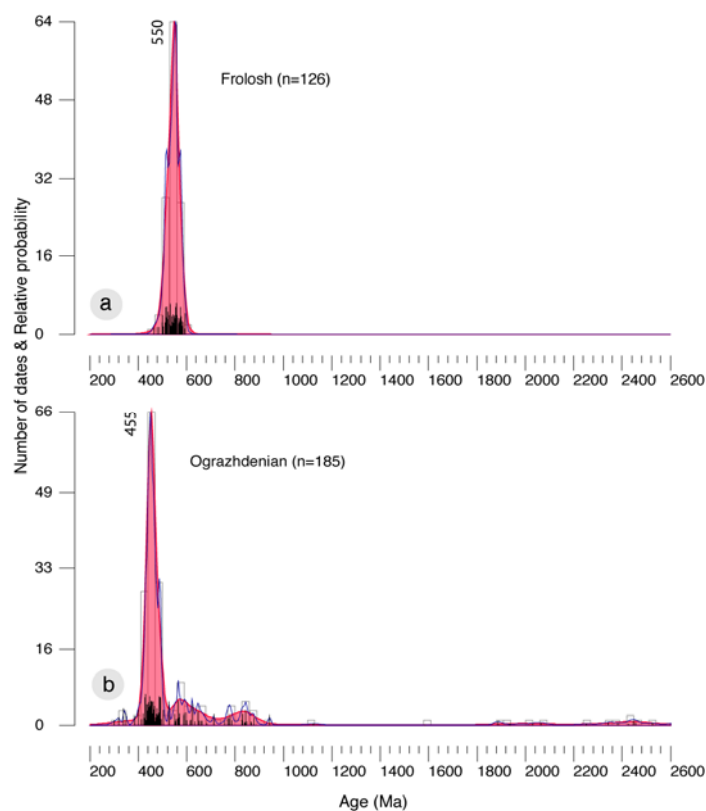


Fig. 11. Frequency distribution of the U-Pb ages of the analyzed zircons

Diagrams show kernel density estimates (reddish curve) overlaid on to probability density plot and histograms (s. Vermeesch, 2012)

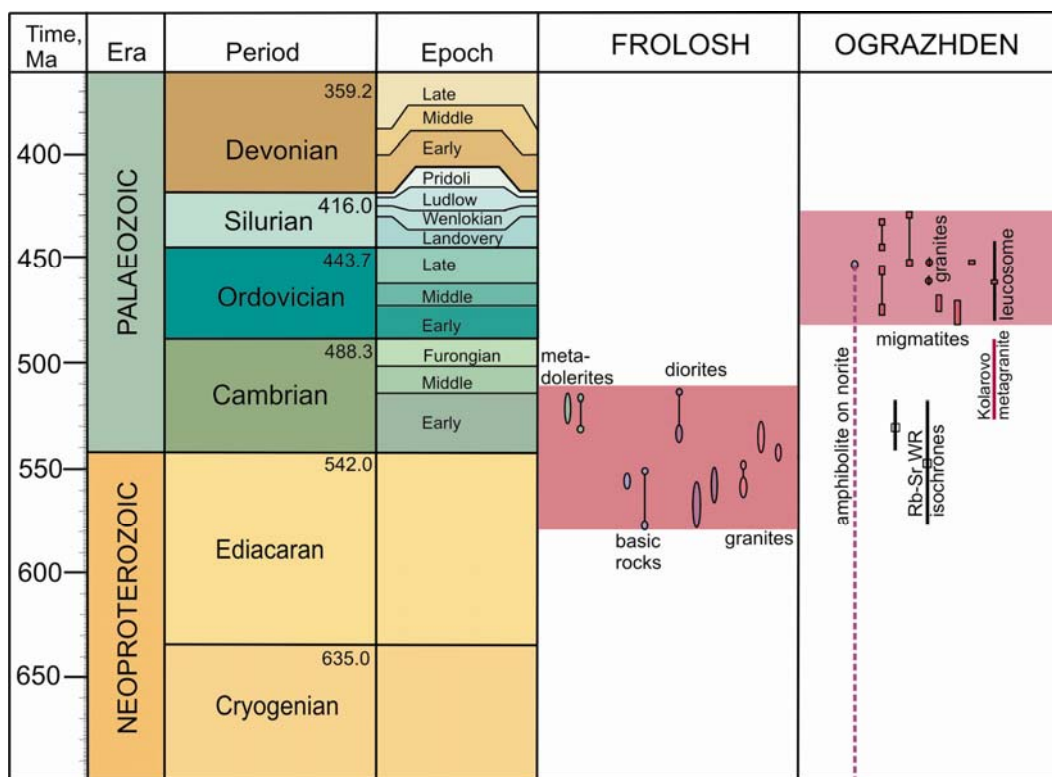


Fig. 12. Geological timescale for the Ediacaran and Early Palaeozoic geochronological evidence on the Ograzhden Unit and the Frolosh Greenstone Belt

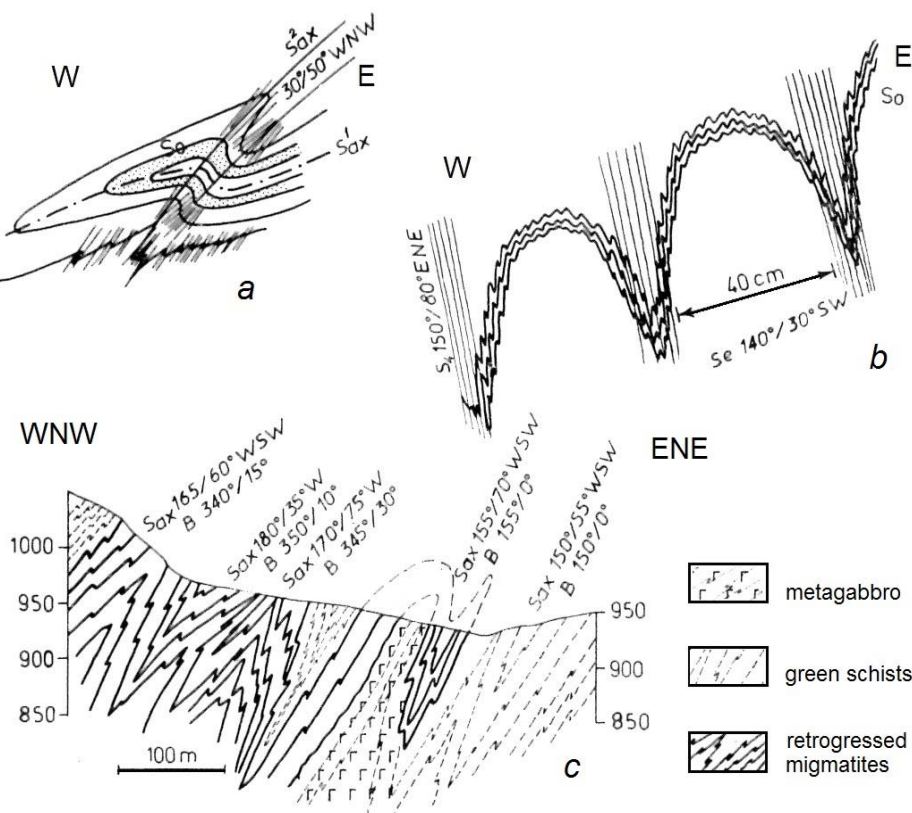


Fig. 13. Ultrametamorphic inliers (field sketches and section): a – F2 coaxial refolding of F1 isoclinal folds; b – F4 folds (Se – enveloping surface); c – detailed section through the diaphthorized migmatite inliers in the uppermost parts of the river Lisiyska (Sax – axial planes; B – fold hinges). Zagorchev (1974, Fig. 2).

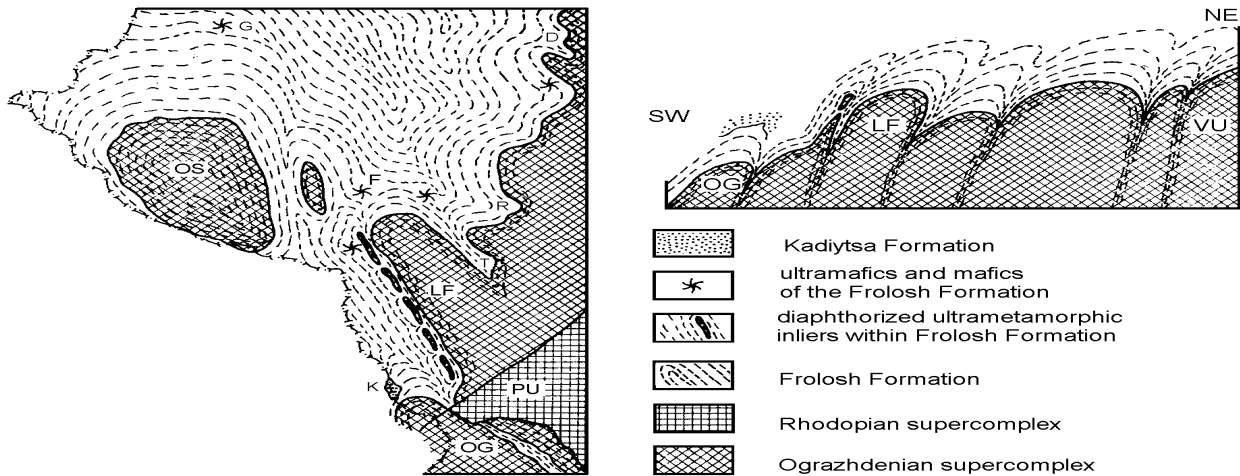


Fig. 14. Relations between the Frolosh complex and the Ograzhdenian supercomplex in SW Bulgaria. After Zagorčev (1987, fig. 3).

4. CONTACTS AND INTERRELATIONS

The problem about the character of the contact between the Frolosh diabase-phyllitoid complex and the underlying Ograzhdenian supercomplex has been subject of long debates in the Bulgarian and Macedonian geological literature. The problem has been reviewed several times since the recognition of the “Diabase-phyllite formation” by Strashimir Dimitrov. The following major opinions have been published (s. Antonov et al., 2001):

(1) Gradual metamorphic transition within a single metamorphic complex, or interlayering of greenschist-facies and amphibolite-facies rocks within a peculiar transition zone (V. T. Despov, S. Belev).

(2) Primary unconformable sedimentary contact later subject of tectonic and metamorphic reworking in greenschist-facies conditions (S. Boyadjiev, D. Kozhoukharov, C. Dabovski, I. Zagorčev, Y. Tenchov, P. Gochev etc.).

(3) Structural and metamorphic unconformity (I. Zagorčev) possibly formed or/and reworked during obduction along the periphery of a “Cadomian” basin.

(4) Overthrust that preceeded the greenschist-facies metamorphism (Zh. Ivanov and co-authors).

(5) Synmetamorphic shear zone (K. Bonev, Zh. Ivanov, L.-E. Ricou) with character of low-angle detachment fault.

(6) West-Bulgarian collisional zone (element of the Variscan Thracian suture) of intensive mostly postmetamorphic and post-Cadomian deformations and metamorphism at the boundary between the continental Thracian composite terrane and the Balkan terrane (I. Haydoutov).

The majority of these hypotheses consider the protolith of the Frolosh diabase-phyllitoid complex as a fragment of oceanic crust or as fragments of an ensimatic arc that contained fragments of oceanic crust. The continental-crust character of the Ograzhdenian complex is considered as an obvious feature. Problems arise because the zircon data define the metamorphism of the Ograzhdenian as being of younger (Ordovician to Silurian) age when compared to the Cadomian age of the rock complexes of the Frolosh Greenstone Belt.

A new view (hypothesis) on the contact zone Frolosh complex/Ograzhdenian supercomplex is proposed with the present paper. Its main points are as follow:

(1) The contact is not a thin “razor-blade” zone but rather a wide zone formed at the expense of both complexes.

(2) The contact zone has been subject of polyphase deformations and metamorphism.

(3) Either primary unconformity, or obduction, or low-angle normal fault or thrust, the contact pre-dated the greenschist-facies metamorphism. This means that the primary contact was of Cadomian age.

(4) During Ordovician to Silurian mid-crustal anatexis in the Ograzhdenian-type basement (infrastructure), its contact zone with the Frolosh complex (superstructure) had a screening effect: deformations and metamorphism in this zone occurred under a steep geothermal gradient, and isolated the superstructure.

For to prove or disprove the hypothesis, we need new detailed structural, petrological, geochemical and isotopic studies on the contact zone.

5. DISCUSSION AND CONCLUSIONS

In the present paper we expose own new evidence, and review the rich facts and ideas published during the last decades.

The dominant ideas (Haydoutov et al., 2012, and older papers by the same authors) in the interpretation of the Frolosh Greenstone Belt consider this here formulated structure as a part of the Iapetus Ocean that developed from MORB ophiolites (ophiolitic fragments in the Frolosh Formation consisting of peridotite and gabbro cumulates, sheeted dyke complex, and pillow lavas, all similar to these in Western Stara-planina Mts.) to the formation and evolution of an ensimatic island arc association (Frolosh Formation s.s., similar to or identical with the Berkovitsa Group, and the Struma diorite complex). Kounov et al. (2012, Fig. 13) and Antić et al. (2015) developed an elaborate concept for the latest Ediacaran times (577 – 540 Ma BP) that considers formation of the Frolosh ophiolites in the Prototethys at the margin with a continental magmatic arc (at the front of Gondwana, with the Struma diorites formed within it), and a Vlasina back-arc basin at the boundary between the continental magmatic arc with Gondwana. Further on, they deduce continuing at the beginning of the Palaeozoic (540–470 Ma BP) a continuous subduction of Baltica under Gondwana (the Peri-Gondwanan region included) with the obduction of the Frolosh ophiolites and the arc collision (with the continental magmatic arc) and the simultaneous transformation of the Vlasina back-arc basin via rifting into a back-arc Rheic Ocean. Furthermore (470–430 Ma BP, Ordovician to Early Silurian), the initial continental magmatic arc of the Struma diorites together with collided fragments from the former Rheic Ocean, and the newly-intruded Ordovician granitoids, formed all together the Serbo-Macedonian massif whereas in its back, the Veles “series” formed into the opening Palaeotethys. The final shape of the region would have been obtained during the Hercynian (380–320 Ma BP) continent-continent collision. This interpretation takes to a certain degree in consideration some previously expressed and forgotten ideas (Aleksić et al., 1988; Rudakov, 1992; Zagorchev, 1998; Zagorchev in Cavazza et al., 2004) about the very complex character of the Prototethys and the whole Northern Peri-Gondwanan Region as also partially reflected recently by Garfunkel (2015).

An extensive palaeodynamic analysis of the evolution of the Northern Peripheral Cadomian

Domain (Peri-Gondwanan Region) is beyond the scope of the present paper. However, we would like to emphasize within the following lines on several important features of the region under consideration.

The northern Peri-Gondwanan Region was apparently (Rudakov, 1992; Nance, Murphy, 1994; Zagorchev, 1998; Neubauer, 2002; v. Raumer et al., 2003; Zagorchev in Cavazza et al., 2004) a mosaic of older continental blocks situated within the complex Prototethys Ocean. The individual crustal fragments drifted within that region, and have been subject of rifting, obduction and/or subduction. The Serbo-Macedonian (Dardanian) unit was one of these continental crustal fragments that had undergone a complex tectonometamorphic evolution prior to the Ediacaran rifting that produced the Frolosh Greenstone Belt (FGB) as a branch of the Prototethys. Late Cadomian (latest Ediacaran – Early Cambrian, c. 550–520 Ma BP) collision resulted in the obduction of the Frolosh Belt together with the volcanic-arc products of the Struma diorite complex over the Ograzhdenian supercomplex of the future Lisiya and Ograzhden fragments. The collision zone had a thickness of at least 1 – 1.5 km (Zagorčev, 1974, 1975), being formed at the expense of both complexes, and had suffered extensive deformations during the Ediacaran collision, when the FGB behaved as a superstructure in respect of the infrastructure (Ograzhdenian supercomplex of the Lisiya core of the Struma Unit, and the Ograzhden Unit). The same relations continued to exist during the Ordovician and Silurian when thermotectonic events with heating and melting (both metatexis and diatexis) within the Ograzhdenian triggered crustal flow and contributed to the formation (Fig. 14) of large brachyanticlines separated by pinched-in synclines. The boundary zone between the two complexes played the role of a screen with a steep geothermal gradient, thus insulating the Frolosh superstructure from the hot Ograzhdenian infrastructure. This role of the boundary zone was maintained also during the Hercynian deformations as recorded and dated in the northern parts of the Struma Unit (s. Zagorchev, 2001; Graf, 2001; Kounov, 2002), and even during the Alpine deformations – e.g., the movements on the Tsurvishte thrust (s. Zagorchev, 2001). However, the ductility contrast between superstructure and infrastructure has changed several times during these events: the relatively higher ductility of the Frolosh metamorphic complex during the Cadomian collision was followed by the Ordovician-Silurian anatexis and flow (higher ductility) of the Ograzhdenian, and during the Her-

cynian and Alpine collisional events the boundary zone between the two complexes was again mostly a higher ductility zone that enabled intense repeated deformations, and epidermal (thin-skinned) thrusting.

In conclusion we wish to stress on the relative paucity in modern detailed evidence, and the need to proceed with extensive complex research within the whole area of the Frolosh Greenstone Belt in the territories of the three countries, with special emphasize on the stratigraphic, petrologic, structural and isotopic studies across the boundary zone with the Ograzhdenian supercomplex to the East,

and within the amphibolite-facies complexes to the West.

Acknowledgements: Field studies and sampling were carried out within the frame of the bilateral project of the Bulgarian Academy of Sciences and the Romanian Academy of Sciences “Principal tectonometamorphic events in the basement of the South Carpathian and the Balkan orogens”. C. Balica and I. Balintoni were financially supported by ID-480 grant and PN-II-ID-PCE-2011-3-0100 project, and G Săbău and E. Neagușescu, by the PN-II-ID-PCE-2011-3-0030 project awarded by CNCS – UEFISCDI units of the Romanian National Authority for Scientific Research.

REFERENCES

- [1] Aleksić, V., Dimitriadis, S., Kalenić, M., Stojanov, R., Zagorčev, I.: Serbo-Macedonian Massif. – In: Zoubek, V., Cogné, J., Kozhoukharov, D., Krautner, H. (eds.). *Precambrian in Younger Fold Belts*. Wiley & Sons; 779–820 (1988).
- [2] Antić, M., Peytcheva, I., Quadt, A. von, Kounov, A., Trivić, B., Serafimovski, T., Tasev, G., Gerdjikov, I., Wetzel, A.: Pre-Alpine evolution of a segment of the North-Gondwanan margin: Geochronological and geochemical evidence from the central Serbo-Macedonian Massif. *Gondwana Research* (2015), doi: 10.1016/j.gr.2015.07.020.
- [3] Antonov, M., Zhelev, V., Pristavova, S., Shipkova, K.: The boundary between the high-grade and the low-grade rocks in a part of SW Bulgaria: review of the ideas and preliminary results. *Review of the Bulgarian Geological Society*, **62**, 1–3; 77–86 (2001) (in Bulgarian, with English summary).
- [4] Bonev, K.: *Limite NW du massif cristallin rhodopien*. Mem. Sciences de la Terre, Univ. Paris et Marie Curie; 269 p. (these de doctorat), 1996.
- [5] Bonev, K., Ivanov, Z., Ricou, L.-E.: Dénuation tectonique au toit du noyau métémorphique Rhodopien-Macédonien: la faille normale ductile de Gabrov Dol (Bulgarie). *Bulletin de la Société géologique de France*, **166**, 1; 49–58 (1995).
- [6] Boyadjiev, S.: On the diabase-phyllitoid complex in Bulgaria. – *Review of the Bulgarian Geological Society*, **31**, 1, 63–74 (1971).
- [7] Cavazza, W., Roure, F., Spakman, W., Stampfli, G., Ziegler, P. (eds.): *The Transmed Atlas*. Part One – Printed volume, 141 pp; Part Two – CD-ROM. Springer, Berlin Hedelberg, 2004.
- [8] Dabovski, C., Boyanov, I., Khrischev, K., Nikolov, T., Sapounov, I., Yanev, Y., Zagorchev, I.: Structure and Alpine evolution of Bulgaria. *Geologica Balcanica*, **32**, 2–4; 9–15 (2002).
- [9] Despov, V.: Geology of the Frolosh area. – *Annual of the Mining and Geology Institute*, **5**, 3; 183–209 (1959) (in Bulgarian).
- [10] Dimitrijević, M. D.: *Geologija Jugoslavije*. Belgrade; 205 p., 1995.
- [11] Dimitrov, S.: Metamorphic and magmatic rocks of Bulgaria. – *Ann. Dir. Geol. and Mine Prospecting*, **A**, **4**, 61–93 (1946) (in Bulgarian).
- [12] Dimitrova, E.: The Struma diorite formation in Stanke Dimitrov area and Lisets Mountain. – *Review of the Bulgarian Geological Society*, **28**, 2; 105–116 (1967) (in Bulgarian).
- [13] Garfunkel, Z.: The relations between Gondwana and the adjacent peripheral Cadomian domain – constrains on the origin, history, and paleogeography of the peripheral domain. *Gondwana Research*, **28**; 1257–1281 (2015).
- [14] Graf, J.: *Alpine tectonics in western Bulgaria: Cretaceous compression of the Kraishte region and Cenozoic exhumation of the crystalline Osogovo-Lisec Complex*. ETH Zurich, Dissertation, No 14238, 197 p., 2001.
- [15] Haydoutov, I.: Precambrian ophiolites, Cambrian island arc, and variscan suture in the South Carpathian – Balkan region. *Geology*, **17**, 905–908 (1989).
- [16] Haydoutov, I.: Peri-Gondwanan terranes in the pre-Early Palaeozoic basement of the region of Bulgaria. *Geologica Balcanica*, **32**, 2–4, 17–20 (2002).
- [17] Haydoutov, I., Pin, C.: Geochemical and Nd isotope characteristics of pre-Variscan ophiolites and meta-igneous rocks from the Struma Diorite Formation in SW Bulgaria. *Geologica Balcanica*, **23**, 51–59 (1993).
- [18] Haydoutov, I., Yanev, S. N.: The Protomoesian micro-continent of the Balkan Peninsula – a peri-Gondwanaland piece. *Tectonophysics*, **272** (2–4), 303–313 (1997).
- [19] Haydoutov, I., Daieva, L., Kolcheva, K.: Dismembered old ophiolites along the Variscan Thracian suture. *Zentralblatt für Geologie und Paläontologie*, Teil I, H. 9/10; 1133–1144 (1994).
- [20] Haydoutov, I., Kolcheva, K., Daieva, L.: The Struma Diorite Formation from Vlahina block, SW Bulgaria. *Review of the Bulgarian Geological Society*, **55**, 9–35 (1994).
- [21] Haydoutov, I., Pristavova, S., Daieva, L.-A.: Some features of the Neoproterozoic-Cambrian Geodynamics in Southeastern Europe. *Comptes-rendus de l'Academie bulgare des sciences*, **63**, 11, 1597–1608 (2010).
- [22] Haydoutov, I., Pristavova, S., Daieva, L.-A.: *Late Neoproterozoic – Early Paleozoic Evolution of the Balkan Terrane (SE Europe) – A probable fragment of Iapetus Ocean*. Mining and Geology University “Sveti Ivan Rilski”, Sofia; 132 pp. 2012 (in Bulgarian, English summary).
- [23] Haydoutov, I., Gochev, P., Kozhoukharov, D., Yanev, S.: Terranes in the Balkan area. — In: Papanikolaou, D. (ed.). IGCP Project No 276. *Terrane maps and terrane*

- descriptions. *Annales géologiques des pays helléniques*, **37**, 479–494 (1997).
- [24] Ivanov, Z., Kolcheva, K., Moskovski, S., Dimov, D.: Des particularités et du caractère de la “formation dia-baso-phyllitoïde”. *Review of the Bulgarian Geological Society*, **48**, 2, 1–24 (1987) (in Bulgarian, with French summary).
- [25] Ivanova, P., Zidarov, N.: Spinel accessories in ultramafic and mafic rocks from Gega ophiolite mélange in Ograzhden Mountain, Southwestern Bulgaria. *National Conference “Geosciences 2010”, Proceedings*, Sofia, pp. 43–44, 2010.
- [26] Kiselinov, H., Peychev, K., Georgiev, S., Peytcheva, I.: New geochronology data on the Lower Cambrian age of the Frolosh Metamorphic Complex (Frolosh Unit) and Kadiytsa Formation – SW Bulgaria. *Bul. Shk. Gjeol.* 1/2014, Special Issue, *Proceedings, XX Congress of the Carpathian-Balkan Geological Association*, Tirana; 200–202, 2014.
- [27] Kounov, A.: *Thermotectonic evolution of Kraishte, Western Bulgaria*. Dissertation ETH 14946, Zurich, 219 p., 2002.
- [28] Kounov, A., Seward, D., Bernoulli, D., Burg, J.-P., Ivanov, Z.: Thermotectonic evolution of an extensional dome: the Cenozoic Osogovo-Lisets core complex (Kraishte zone, western Bulgaria). *Int J Earth Sci (Geol Rundsch)*, **93**, 1008–1024 (2004).
- [29] Kounov, A., Graf, J., Quadt, A. v., Bernoulli, D., Burg, J.-P., Seward, D., Ivanov, Z., Fanning, M.: Evidence for a “Cadmian” ophiolite and magmatic-arc complex in SW Bulgaria. *Precambrian Research*, 212–213; 275–295 (2012).
- [30] Kozhoukharov, D.: Interregional correlations of the Precambrian in the southern parts of the Balkan Peninsula. *Geologica Carpathica*, **37**, 3; 317–333 (1986).
- [31] Kräutner, H.-G., Krstić, B.: Alpine and Pre-Alpine structural units within the Southern Carpathians and the Eastern Balkanides. In: *17th Congr. Carp.-Balk. Geol. Assoc.*, Bratislava, 2002.
- [32] Krstić, B., Karamata, S., Miličević, V.: The Carpatho-Balkanide terranes – a correlation. In: Knežević, V., Krstić, B. (eds.) *Terranes of Serbia*. University of Belgrade, Belgrade; 71–76, 1996.
- [33] Lakova, I.: Additional palynological data about the age of the Razchka Formation, Osogovo Mt., SW Bulgaria. – *Geologica Balcanica*, **27**, 1, 36 (1997).
- [34] Lakova, I., I. Zagorčev, N. Vardev, M. Aleksandrov, R. Stojanov.: Organic-walled microfossils of Wenlockian to Lower Devonian age from Razca Formation and its equivalents from the Elešnica allochthon (Osogovo Mts.). *Geologica Balcanica*, **25**, 1, 20 (1995).
- [35] Macheva, L., Titorenko, R., Zidarov, N.: Kyanite-staurolite-garnet-bearing schists from Ograzhden Mountain, SW Bulgaria – Metapelites or Orthoschists? In: *Geosciences 2005*, Sofia, 138–141.
- [36] Macheva, L., Peytcheva, I., von Quadt, A. von, Zidarov, N., Tarassova, E.: Petrological, geochemical and isotope features of Lozen metagranite, Belasitsa Mountain – evidence for widespread distribution of Ordovician meta-granitoids in the Serbo-Macedonian Massif, SW Bulgaria. In: *Geosciences 2006*, Sofia; 209–212.
- [37] Milovanov, P., Klimov, I., Zhelev, V., Petrov, I., Sinnovski, D., Valev, V., Ilieva, E., Naydenov, E.: *Geological map of the Republic of Bulgaria 1:50000. Map sheet K-34-70-V (Rakovo), and Explanatory note*. Geocomplex, Sofia; 76 p. 2008.
- [38] Milovanov, P., Petrov, I., Klimov, I., Zhelev, V., Sinnovski, D., Valev, V., Ilieva, E., Naydenov, E.: *Geological map of the Republic of Bulgaria 1:50000. Map sheet K-34-70-G (Vaksevo), and Explanatory note*. Geocomplex, Sofia; 66 p. 2008.
- [39] Milovanov, P., Petrov, I., Valev, V., Marinova, A., Klimov, I., Sinnovski, D., Ichev, M., Pristavova, S., Ilieva, E.: *Geological map of the Republic of Bulgaria 1:50000. Map sheets K-34-82-B (Delchevo), and K-34-83-A (Simitli); and Explanatory note*. Geocomplex, Sofia; 108 p. 2008.
- [40] Milovanov, P., Petrov, I., Valev, V., Marinova, A., Klimov, I., Sinnovski, D., Ichev, M., Pristavova, S., Ilieva, E.: *Geological map of the Republic of Bulgaria 1:50000. Map sheets K-34-82-G (Berovo), and K-34-83-V (Kresna); and Explanatory note*. Geocomplex, Sofia; 76 p. 2008.
- [41] Nance, R. D., Murphy, J. B.: Contrasting basement isotopic signatures and the palinspastic restoration of peripheral orogens: example from the Neoproterozoic Avalonian–Cadomian belt. *Geology*, **22**; 617–620 (1994).
- [42] Nenova, P., Marinova, I.: New data on the serpentized ultrabasic body at the village of Kamena, Belassitsa Mountain, SW Bulgaria. *“Geosciences 2007”*, 99–100 (in Bulgarian).
- [43] Nenova, P., Zidarov, N.: Eclogites from Maleshevská Mountain, SW Bulgaria. *“60 Years Education in Geology”*, Publ. House “St. Kl. Ohridski”, Sofia, 109–114, 2008.
- [44] Nenova, P., Zidarov, N.: Mineral Composition and Peculiarities of Megacrystal Pyroxenites from Ograzhden Mountain. *Scientific session “Development of Bulgarian Mineralogy” – 80th anniversary of acad. I. Kostov*, September 23–24, 1993, p. 44 (in Bulgarian).
- [45] Neubauer, F.: Evolution of the late Neoproterozoic to early Paleozoic tectonic elements in Central and Southeast European Alpine mountain belts: review and synthesis. *Tectonophysics*, **352**; 87–103 (2002).
- [46] Peytcheva, I., E. Tarassova, A. v. Quadt, M. Tarassov, N. Zidarov, V. Andreichev: Petrology, Geochemistry and Age Dating of Igralishte Pluton in SW Bulgaria: Implications for the Permian-Triassic Tectonomagmatic Evolution of the Region. In: *Proc. 62nd Geological Kurultai of Turkey*, April 13–17, 2009. MTA-Ankara, Türkiye, p. 653.
- [47] Peytcheva, I., Quadt, A. v., Tarassov, M., Zidarov, N., Tarassova, E., Andreichev, V.: Timing of Igralishte Pluton in Ograzhden Mountain, SW Bulgaria. *Geologica Balcanica*, **38**, 1–3, 5–14 (2009).
- [48] Peytcheva, I., A. v. Quadt, R. Titorenko, N. Zidarov, E. Tarassova: Skrut granitoides from Belassitsa Mountain, SW Bulgaria: Constraints from isotope geochronological and geochemical zircon data. *Geosciences 2005*, Sofia; 109–122.
- [49] Pristavova, S., M. Ichev, M. Komsalova: Garnet-kyanite schists from the Ograzhden Mountain, SW Bulgaria. *Geochemistry, Mineralogy and Petrology*, **45**, 97–107 (2007).
- [50] Ricou, L.-E., Burg, J.-P., Godfriaux, I., Ivanov, Z.: Rhodope and Vardar: the metamorphic and the olistostromic paired belts related to the Cretaceous subduction under Europe. *Geodynamica Acta*, **11**, 6; 285–309 (1998).
- [51] Rudakov, S. G.: Specific features in the evolution of the Carpathians and the Balkan in the confines of the European Prototethys. *Geologica Balcanica*, **22**, 6, 3–20 (1992).

- [52] Spassov, H.: Stratigraphy of the Ordovician and Silurian in the core of Svoge anticline. *Travaux sur la géologie de la Bulgarie*, ser. *Stratigraphie et Tectonique*, **1**; 161–202 (1960) (in Bulgarian).
- [53] Spassov, H.: Stratigraphy of the Devonian in Southwestern Bulgaria. *Bulletin of the Geological Institute*, ser. *Stratigraphy and Lithology*, **22**, 5–38 (1973) (in Bulgarian).
- [54] Stefanov, A., Dimitrov, C.: Geological studies in the Kyustendil District. *Review of the Bulgarian Geological Society*, **8**, 3; 1–28 (1936) (in Bulgarian).
- [55] Stojanov, R., Zagorchev, I., Dumurdanov, N., Aleksandrov, M.: Palaeozoic correlations in the border areas of Macedonia and SW Bulgaria. Boev, B., Serafimovski, T. (eds.) *Proceeding, Magmatism, metamorphism and metallocogeny of the Vardar Zone and Serbo-Macedonian Massif*, Štip; 209–214, 1997.
- [56] Titorenkova, R., Macheva, L., Zidarov, N., Quadt, A. von, Peytcheva, I.: Metagranites from SW Bulgaria as a part of the Neoproterozoic to early Paleozoic system in Europe: New Insight from Zircon Typology, U-Pb Isotope Data and Hf-tracing. *EGS-AGU-EUG Joint Assembly, Abstracts* from the meeting held in Nice, France, April 6–11, 2003.
- [57] Vermeesch, P.: On the visualization of detrital age distributions. *Chemical Geology*, **312–313**, 190–194 (2012).
- [58] Von Raumer, J., Stampfli, G. M., Bussy, F.: Gondwanaderived microcontinents — the constituents of the Variscan and Alpine collisional orogens. *Tectonophysics*, **365**, 7–22 (2003).
- [59] Zagorčev, I.: Contribution to the geology of the area west of Boboshevo, Kyustendil District. *Review of Bulgarian Geological Society*, **27**, 117–126 (1966) (in Bulgarian, with English summary).
- [60] Zagorčev, I.: On the tectonic style of the Pre-Cambrian fragments in SW Bulgaria. – *Carpathian-Balkan Geological Association, VIII Congress, Belgrade, Reports, Geotectonics*; 207–212, 1967.
- [61] Zagorčev, I.: Ultrametamorphic inliers within the diabasphyllitoid complex, Vlahina block, SW Bulgaria. *C.-r. Acad. bulg. Sci.*, **27**, 9, 1255–1258 (1974).
- [62] Zagorčev, I.: On the structural interrelations between the diabas-phyllitoid complex and the lower (ultrametamorphic) Precambrian complex in SW Bulgaria. *Proc. X Congr. CBGA 1973, Sect. VI*, 221–227, 1975.
- [63] Zagorčev, I.: Tectonic, metamorphic and magmatic markers in the polycyclic ultrametamorphic Ograzhdenian complex. *Geologica Balcanica*, **6**, 2; 17–33 (1976).
- [64] Zagorčev, I.: Structure of the Amphibolitic Series in the Vlahina Block (Southwest Bulgaria). *Geotectonics, Tectonophysics, Geodynamics* (Sofia), **5**, 29–56 (1976) (in Bulgarian, with English summary).
- [65] Zagorčev, I.: Structure of the Gneiss-Migmatitic Series in Vlahina Block (Southwest Bulgaria). *Geotectonics, Tectonophysics, Geodynamics* (Sofia), **13**; 29–44 (1981) (in Bulgarian, with English summary).
- [66] Zagorčev, I.: Early Alpine deformations within the Poletintsi-Skrino fault zone. 4. Shipochano anticline. *Review of the Bulgarian Geological Society*, **46**, 3, 287–298 (1985).
- [67] Zagorčev, I.: Stratigraphy of the Diabase-phyllitoid complex in Southwest Bulgaria. *Geologica Balcanica*, **17**, 3, 3–14 (1987) (in Russian, with English abstract).
- [68] Zagorčev, I.: Troskovo Amphibolitic Group (Ograzhdenian Supergroup, Precambrian) in Vlahina Mountain, SW Bulgaria. *C.-R. Bulg. Acad. Sci.*, **42**, 11; 67–70 (1989) (in Russian).
- [69] Zagorčev, I.: *Geological map of Bulgaria. Sheet Delčovo*. M 1:100 000. MTS, Troyan (1989).
- [70] Zagorčev, I., Bončeva, I.: Indications for Devonian basic volcanism in South-West Bulgaria. *Geologica Balcanica*, **18**, 4, 55–63 (1988).
- [71] Zagorčev, I.: Complex shear and flow in the Ograzhdenian Supergroup, Southern Bulgaria. *Zeitschrift für geologische Wissenschaften*, **24**, 3/4; 255–271 (1996).
- [72] Zagorčev, I.: Rhodope controversies. *Episodes*, **21**, 3, 159–168 (1998).
- [73] Zagorčev, I.: Rhodope and Vardar: the metamorphic and the olistostromic paired belts related to the Cretaceous subduction under Europe. Comment: Rhodope facts and Tethys self-delusions. *Geodynamica Acta*, **1**, 55–59 (2000).
- [74] Zagorčev, I.: Introduction to the geology of SW Bulgaria: an overview. *Geologica Balcanica*, **31**, 1–2, 3–52 (2001).
- [75] Zagorčev, I.: Cadomian basement on the Balkan Peninsula and its role for the Phanerozoic geodynamics. In: Ioane, D. (ed.) *The Fourth Stephan Mueller Conference. Book of Abstracts, Retezat Mountains, Romania*; 68–70, 2003.
- [76] Zagorčev, I.: Polymetamorphic complexes in the eastern parts of the Balkan Peninsula: 600 Ma of geodynamic evolution. American Geophysical Union, *Eos Transactions AGU*, 88 (52), Fall Meet. Suppl., Abstract V13A–1142 (2007).
- [77] Zagorčev, I.: Amphibolite-facies metamorphic complexes in Bulgaria and Precambrian geodynamics: controversies and “state of the art”. *Geologica Balcanica*, **37**, 1–2, 33–46 (2008).
- [78] Zagorčev, I.: Rhodope evolution in the heart of Balkan geology. in: *Proceedings of the XVI Serbian Geological Congress, Donji Milanovac, 22–25. 05. 2014*; 43–48, 2014.
- [79] Zagorčev, I., Ruseva, M.: *Geological map of Bulgaria 1:100000. Sheet Kriva Palanka and Kyustendil*. MTS, Troyan, 1991.
- [80] Zagorčev, I., Milovanović, D.: Deformations and metamorphism in the eastern parts of the Serbo-Macedonian Massif. In: *Proceedings of the 18th Congress of the Carpathian-Balkan Geological Association*, Belgrade; 670–673, 2006.
- [81] Zagorčev, I., Dabovski, C., Nikolov, T. (eds.): *Geology of Bulgaria. Vol. 2. Part 5. Mesozoic Geology*. Acad. Publ. House “Prof. Marin Drinov”, Sofia, 2009.
- [82] Zagorčev, I., Balica, C., Bayanova, T. B., Kozhoukharova, E. S., Balintoni, I. C., Mitrofanov, F. P., Lyalina, B. V., Săbău, G., Negulescu, E.: Precambrian metabasic relicts in the Ograzhdenian supercomplex, Gorna Ribnitsa Village, Serbo-Macedonian massif, Southwest Bulgaria. *Bul. Shk. Gjeol.* 1/2014, Special Issue, *Proceedings, XX Congress of the Carpathian-Balkan Geological Association*, Tirana; 224–227, 2014.
- [83] Zagorčev, I., Balica, C., Balintoni, I., Kozhoukharova, E., Dumitrescu, R., Sabau, G., Negulescu, E.: New Isotopic Data on the Metamorphic Rocks in SW Bulgaria. – *3rd International Symposium on the Geology of the Black Sea Region*, Bucharest, 223–225, 2011.
- [84] Zagorčev, I., Balica, C., Balintoni, I., Kozhoukharova, E., Dumitrescu, R., Sabau, G., Negulescu, E.: New isotopic data on the Cadomian age of the Frolosh metamorphic complex and the Struma diorite complex. *Geosciences’2011*, Sofia, 77–78, 2011.
- [85] Zagorčev, I., C. Balica, I. Balintoni, E. Kozhoukharova, G. Săbău, R. Dumitrescu, E. Negulescu: Isotopic data on

- the age of the Krupnik granite pluton and its host rocks, Kresna horst, Krupnik Mountain, SW Bulgaria. *C.-r. Acad. Bulg. Sci.*, **65**, 7, 977–984 (2012).
- [86] Zagorchev, I., C. Balica, I. Balintoni, E. Kozhoukharova, G. Săbău, E. Negulescu: Palaeozoic evolution of the Ograzhden Unit (Serbo-Macedonian Massif, Bulgaria and Macedonia). *Proceedings. 2nd Congress of the Geologists of Macedonia*; 13–18, 2012.
- [87] Zidarov, N. G., Nenova, P. I.: Basic and Ultrabasic Rocks and Related Eclogites from the Serbo-Macedonian Massif (South-Western Bulgaria). *Geol. Soc. Greece (XV Congress of KBGA, September 17–20. 1995)*, Sp. Publ., no. 4/2, 619–626, 1995.
- [88] Zidarov, N., Nenova, P.: Evidence of Ultrahigh-pressure Metamorphism in the Ograzhden Blok of the Serbo-Macedonian Massif, *6th Congress of the Bulg. Geol. Society, October 24–25, 1996, Sofia, Bulgaria*, Abstracts, 21–22, 1996 (in Bulgarian).
- [89] Zidarov, N., Nenova, P.: Mineral Equilibrium before the Eclogitic Stage of Metamorphic Evolution of Gabbro Noritic Dyke's Complex from SW Bulgaria. *Jubilee Scientific Session "Problems of Mineral Genesis", 85th Anniversary of Acad. I. Kostov, January 21–22. 1999*. Abstracts (in Bulgarian).
- [90] Zidarov, N., Andreichev, V., Peytcheva, I.: Rb-Sr Isotope Data on Variscan and Alpine Polymetamorphic Evolution of the Granitoids from the Ograzhden Unit in SW Bulgaria. – In: *Geosciences 2009*, Sofia, 27–28.
- [91] Zidarov, N. G., Nenova, P. I., Dimov, V. I.: Spinel Clinopyroxenites with Diopside Megacryst from SW Bulgaria: Phase Composition and Formation Conditions. *IMA, 16th General Meeting, Pisa, Italy, September 4–9. 1994*, Abstracts, 462–463.
- [92] Zidarov, N. G., Nenova, P. I., Dimov, V. I.: Coesite in Kyanite Eclogite of Ograzhden Mts, SW Bulgaria. *Compt. Rend. Acad. Bulg. Sci.*, **48**, 11–12, 59–62 (1995).
- [93] Zidarov, N., Tarassova, E., Peytcheva, I., Quadt, A. von, Andreichev, V., Titorenkova, R.: Petrology, geochemistry and age dating of Skrut granitoids – new evidence for Early Triassic magmatism in Belasitsa Mountain (SW Bulgaria). *Geologica Balcanica*, **36**, 1–2; 17–29 (2007).
- [94] Zidarov, N., Peytcheva, I., Quadt, A. von, Macheva, L., Nenova, P.: Distinction of crustal terranes in Ograzhden and Belasitsa Mountains (Serbo-Macedonian Massif, SW Bulgaria) based on U-Pb conventional and LA-ICP-MS dating of zircons. *Annual Report # 13, Central Laboratory of Mineralogy and Crystallography "Acad. Ivan Kostov", Sofia*; 18–19 (2007).

Резиме

КАДОМИСКА И ПОСТ-КАДОМИСКА ТЕКТОНИКА ЗАПАДНО ОД РОДОПСКИОТ МАСИВ – ФРОЛОШ ПОЈАС НА ЗЕЛЕНИ КАРПИ И ОГРАЖДЕНСКИ МЕТАМОРФЕН СУПЕРКОМПЛЕКС

Иван Загорчев¹, Константин Балика², Евгенија Кожухарова¹,
Јоан Кориолан Балинтони², Гаврил Сабау³, Елена Негулеску³

¹Бугарска академија на науките, Софија, Бугарија
²Универзитет Бабеш-Болаи, Клуј-Найок, Романија
³Геолошки институт на Романија, Букурешт, Романија
i_zagorchev@geology.bas.bg

Клучни зборови: српско-македонски масив; огражденска единица; појас на зелени карпи Фролош; родопски масив; доцен протерозоик; палеозојска тектоника

Појасот на зелени карпи Фролош (FGB) се протега на растојание поголемо од 200 km на териториите на Бугарија, Македонија и Србија. Се состои од различни карпи на фацијата зелени шкрилци (актинолитски шкрилци, филити, Са-шкрилци, нечисти мермери, метапесочници, медини бази, масивни зелени карпи и др.) од метаморфниот комплекс Фролош со метабазити (вклучително лерзолити) и области на постари карпи опкружени со помлади (ретроградни момирочки гнајсеви и мигматити) од огражденскиот суперкомплекс. Комплексот е пробиен од тела на габрови (наместа со ултрабазични кумулати), диорити до гранити (диоритска формација Струма). U-Pb-проучувањата на циркони покажале кадомиска старост со временски период помеѓу сса. 574 и 517 Ma. Комплексот Фролош ги покрива ултраметаморфитите (мигматизирани гнајсеви и амфиболити; турмалинско-биотитски шкрилци; кварц-фелдспатски гнајсеви; лековидни тела на метапериодотити до норити) на огражденскиот суперкомплекс. Огражденските карпи се испресечени со дијатектички метагранити препокриени со метаморфизам на амфиболитска фација. Доминантната U-Pb-старост варира помеѓу 470 и 430 Ma.

Контактот помеѓу комплексот Фролош и огражденскиот суперкомплекс бил предмет на долга дискусија и контроверзни интерпретации. Сега ние го потенцираме повеќефазниот развој на двата комплекса, како што е докажано со теренските податоци и изотопната старост. Огражденскиот суперкомплекс бил подложен на прекамбрискиот тектонометаморфизам, што е докажано со изохроните податоци за Rb-Sr на цела карпа и цирконските податоци за U-Pb на реликти. Ордовициските до силурски анектетити (метатектичка мигматизација, дијатексис) се интрудирани од пермо-тријаски гранити. Контактот помеѓу огражденскиот суперкомплекс и покровниот комплекс Фролош се смета за моќна комплексна зона на повеќефазен тектонометаморфен развој повеќе отколку остра површина со еднофазно потекло. Како граница помеѓу супратекtonика и инфраструктура, таа одиграла важна улога во времето на фанерозоик и послужила како екран со висок термален градиент за време на ордовициско-силурскиот антекексис и метаморфизам во огражденскиот суперкомплекс. За да се верифицира оваа хипотеза, неопходни се нови детални структурни и изотопни проучувања.

Annex 1

Isotope data for the zircons in sample 294B, metadolerite, road cuttings between the villages of Tsurvishte and Frolosh, near the Kopriven River

	U (ppm)	Isotope ratios						Apparent ages						Best age		Conc (%)			
		$^{207}\text{Pb}^*/^{235}\text{U}^*$	$\pm (\%)$	$^{206}\text{Pb}^*/^{238}\text{U}$	$\pm (\%)$	error corr.	$^{206}\text{Pb}^*/^{238}\text{U}^*$	$\pm (\text{Ma})$	$^{207}\text{Pb}^*/^{235}\text{U}$	$\pm (\text{Ma})$	$^{206}\text{Pb}^*/^{207}\text{Pb}^*$	$\pm (\text{Ma})$	(Ma)	$\pm (\text{Ma})$					
RO294B-2	251	73128	1,7	17,3352	4,9	0,6838	5,3	0,0860	1,9	0,36	531,7	9,7	529,1	21,7	517,8	107,9	531,7	9,7	100,5
RO294B-3	905	257628	7,7	17,3036	1,9	0,6825	2,2	0,0857	1,1	0,52	529,8	5,8	528,3	9,1	521,8	41,5	529,8	5,8	100,3
RO294B-4	356	129286	8,3	17,0259	2,5	0,7100	2,8	0,0877	1,3	0,47	541,8	6,8	544,7	11,9	557,2	54,3	541,8	6,8	99,5
RO294B-5	739	57614	2,2	17,0820	3,8	0,6500	4,3	0,0805	2,1	0,49	499,3	10,1	508,5	17,4	550,1	82,8	499,3	10,1	98,2
RO294B-6	199	24528	4,3	17,0609	6,4	0,6834	6,5	0,0846	0,7	0,11	523,3	3,7	528,8	26,6	552,8	140,2	523,3	3,7	99,0
RO294B-7	760	91858	2,2	16,8605	2,0	0,6656	2,9	0,0814	2,2	0,74	504,4	10,5	518,0	11,9	578,5	43,3	504,4	10,5	97,4
RO294B-8	613	140488	3,7	17,2899	2,3	0,6873	2,3	0,0862	0,5	0,23	532,9	2,8	531,2	9,7	523,6	50,0	532,9	2,8	100,3
RO294B-9	307	114384	5,0	16,8408	5,5	0,6921	5,7	0,0845	1,2	0,21	523,1	5,9	534,0	23,5	581,0	120,2	523,1	5,9	98,0
RO294B-10	373	40726	1,8	16,8329	3,4	0,7104	4,6	0,0867	3,1	0,67	536,2	15,8	545,0	19,3	582,1	73,5	536,2	15,8	98,4
RO294B-11	463	200114	4,7	17,2119	2,0	0,6695	2,3	0,0836	1,0	0,44	517,4	5,0	520,4	9,2	533,5	44,3	517,4	5,0	99,4
RO294B-12	187	42006	1,4	17,1110	5,1	0,7235	5,7	0,0898	2,5	0,45	554,3	13,4	552,7	24,2	546,3	111,0	554,3	13,4	100,3
RO294B-13	53	14338	2,2	16,4437	11,4	0,7753	11,4	0,0925	1,2	0,11	570,1	6,6	582,8	50,7	632,7	245,4	570,1	6,6	97,8
RO294B-14	23	3076	1,9	16,7300	32,6	0,7249	32,7	0,0880	2,2	0,07	543,5	11,3	553,6	140,4	595,4	724,7	543,5	11,3	98,2
RO294B-15	390	32586	2,1	17,3531	2,7	0,7015	3,1	0,0883	1,5	0,47	545,4	7,6	539,7	12,8	515,6	59,4	545,4	7,6	101,1
RO294B-16	1507	47002	2,9	16,8346	1,5	0,6422	2,9	0,0784	2,5	0,85	486,6	11,6	503,6	11,6	581,8	33,4	486,6	11,6	96,6
RO294B-17	585	116230	5,2	17,3750	2,4	0,6856	2,5	0,0864	1,0	0,38	534,2	4,9	530,1	10,5	512,8	51,7	534,2	4,9	100,8
RO294B-18	743	196960	3,0	17,5077	1,3	0,6596	1,4	0,0838	0,6	0,43	518,5	3,0	514,4	5,6	496,1	27,6	518,5	3,0	100,8
RO294B-19	587	44552	1,6	17,1163	2,2	0,7259	2,3	0,0901	0,6	0,26	556,2	3,1	554,1	9,6	545,7	47,5	556,2	3,1	100,4
RO294B-20	330	27336	3,3	17,7075	2,0	0,6423	2,4	0,0825	1,4	0,58	511,0	7,0	503,7	9,7	471,0	43,9	511,0	7,0	101,4
RO294B-21	353	123576	5,3	17,3948	1,8	0,6601	3,3	0,0833	2,7	0,83	515,7	13,4	514,7	13,2	510,3	40,0	515,7	13,4	100,2
RO294B-22	619	114418	2,2	16,7396	1,2	0,7688	2,1	0,0933	1,8	0,84	575,2	9,8	579,1	9,4	594,1	24,9	575,2	9,8	99,3
RO294B-23	551	109954	3,9	17,3566	2,7	0,6917	2,8	0,0871	0,9	0,32	538,2	4,6	533,8	11,7	515,1	58,9	538,2	4,6	100,8
RO294B-24	856	452474	4,3	17,3409	1,2	0,6682	1,9	0,0840	1,4	0,75	520,2	7,0	519,6	7,6	517,1	27,2	520,2	7,0	100,1
RO294B-25	219	35926	4,5	17,4072	3,2	0,6769	3,4	0,0855	1,1	0,32	528,6	5,4	524,9	13,8	508,8	70,0	528,6	5,4	100,7
RO294B-26	222	21836	3,3	17,5276	5,2	0,6614	7,3	0,0841	5,1	0,70	520,4	25,5	515,4	29,6	493,6	115,7	520,4	25,5	101,0
RO294B-27	1114	114178	2,2	17,2495	0,8	0,6657	2,3	0,0833	2,1	0,94	515,7	10,6	518,1	9,2	528,7	16,5	515,7	10,6	99,5

Annex 2

Isotopic data for sample 295BF, basic enclave in Struma diorite, road cuttings near the village of Tsurvishte

	U, ppm	$^{206}\text{Pb}/^{204}\text{Pb}$	U/Th	$^{206}\text{Pb}^*/^{207}\text{Pb}^*$	\pm (%)	Isotope ratios				Apparent ages				Best age		Conc (%)			
						$^{207}\text{Pb}^*/^{235}\text{U}^*$	\pm (%)	$^{206}\text{Pb}^*/^{238}\text{U}$	\pm (%)	error corr.	$^{206}\text{Pb}^*/^{238}\text{U}^*$	\pm (Ma)	$^{207}\text{Pb}^*/^{235}\text{U}$	\pm (Ma)	$^{206}\text{Pb}^*/^{207}\text{Pb}^*$	\pm (Ma)			
RO295BF-1	61	5200	1.2	16.7138	11.7	0.7467	11.9	0.0905	2.2	0.19	558.6	11.8	566.3	51.6	597.5	253.5	558.6	11.8	93.5
RO295BF-2	79	8016	1.0	16.1729	7.0	0.7580	7.1	0.0889	1.5	0.21	549.1	7.9	572.9	31.2	668.3	149.2	549.1	7.9	82.2
RO295BF-3	44	34012	1.7	15.0004	10.3	0.8622	10.3	0.0938	0.8	0.08	578.0	4.6	631.3	48.6	827.3	215.3	578.0	4.6	69.9
RO295BF-5	181	12152	0.9	16.2255	6.3	0.7608	6.3	0.0895	1.1	0.17	552.8	5.7	574.5	27.9	661.3	134.1	552.8	5.7	83.6
RO295BF-6	116	31002	1.1	17.3456	5.7	0.7377	5.9	0.0928	1.3	0.22	572.1	7.1	561.1	25.3	516.5	125.7	572.1	7.1	110.8
RO295BF-7	79	8644	1.5	17.1206	8.1	0.7249	8.5	0.0900	2.8	0.33	555.6	14.9	553.5	36.4	545.2	176.3	555.6	14.9	101.9
RO295BF-8	111	18574	1.1	16.1973	8.0	0.7455	9.6	0.0876	5.4	0.56	541.2	28.1	565.6	41.7	665.1	170.7	541.2	28.1	81.4
RO295BF-10	163	5000	0.9	16.7995	5.3	0.7119	5.6	0.0867	2.0	0.35	536.2	10.2	545.9	23.8	586.4	114.5	536.2	10.2	91.4
RO295BF-11	78	11180	1.4	17.0459	12.4	0.7227	12.4	0.0894	0.9	0.07	551.7	4.7	552.3	52.9	554.7	270.9	551.7	4.7	99.5
RO295BF-12	115	37586	0.9	17.8796	5.5	0.6747	5.8	0.0875	1.8	0.31	540.7	9.2	523.6	23.7	449.6	122.6	540.7	9.2	120.3
RO295BF-13	116	30344	1.0	17.6407	7.0	0.6883	7.1	0.0881	1.1	0.15	544.1	5.6	531.8	29.2	479.4	154.2	544.1	5.6	113.5
RO295BF-14	102	18384	1.2	17.2108	8.8	0.6906	9.3	0.0862	3.1	0.33	533.0	15.7	533.2	38.7	533.6	193.0	533.0	15.7	99.9
RO295BF-15	75	18672	1.4	16.6989	10.6	0.7336	10.8	0.0888	2.0	0.19	548.7	10.6	558.7	46.5	599.4	230.7	548.7	10.6	91.5
RO295BF-16	112	14072	1.2	17.1188	5.4	0.7263	5.5	0.0902	0.7	0.13	556.5	3.7	554.4	23.4	545.4	118.7	556.5	3.7	102.1
RO295BF-17	74	9490	1.2	16.3839	9.7	0.7841	9.9	0.0932	1.5	0.15	574.2	8.3	587.8	44.0	640.5	209.8	574.2	8.3	89.7
RO295BF-18	92	44294	2.3	15.9841	7.2	0.7610	7.3	0.0882	1.4	0.19	545.0	7.3	574.6	32.1	693.4	153.2	545.0	7.3	78.6
RO295BF-19	56	20236	1.3	15.9113	18.4	0.7724	18.4	0.0891	1.4	0.08	550.4	7.6	581.1	81.7	703.1	394.2	550.4	7.6	78.3
RO295BF-20	54	18412	1.9	16.7815	12.4	0.7357	12.7	0.0895	2.4	0.19	552.8	12.7	559.9	54.5	588.7	270.6	552.8	12.7	93.9
RO295BF-21	70	11982	1.9	15.3656	7.7	0.8226	8.0	0.0917	1.8	0.23	565.4	10.0	609.5	36.5	776.9	163.0	565.4	10.0	72.8
RO295BF-22	81	60424	0.7	16.1675	9.9	0.7724	10.1	0.0906	1.6	0.16	558.9	8.8	581.1	44.5	669.0	212.9	558.9	8.8	83.5
RO295BF-23	40	6958	1.5	17.7904	15.8	0.6898	16.1	0.0890	3.4	0.21	549.6	18.1	532.7	67.0	460.6	351.7	549.6	18.1	119.3
RO295BF-24	65	90746	2.2	16.5125	7.4	0.7817	7.6	0.0936	1.9	0.25	576.9	10.4	586.5	34.0	623.6	159.8	576.9	10.4	92.5
RO295BF-25	82	33836	1.5	15.9447	6.1	0.7736	6.2	0.0895	1.0	0.16	552.3	5.3	581.8	27.5	698.6	130.6	552.3	5.3	79.1

	U, ppm	Isotope ratios					Apparent ages					Best age		Conc (%)					
		$^{206}\text{Pb} / ^{204}\text{Pb}$	U/Th	$^{206}\text{Pb}^* / ^{207}\text{Pb}^*$	$\pm (\%)$	$^{207}\text{Pb}^* / ^{235}\text{U}^*$	$\pm (\%)$	$^{206}\text{Pb}^* / ^{238}\text{U}$	$\pm (\%)$	error corr.	$^{206}\text{Pb}^* / ^{238}\text{U}^*$	$\pm (\text{Ma})$	$^{207}\text{Pb}^* / ^{235}\text{U}$	$\pm (\text{Ma})$	$^{206}\text{Pb}^* / ^{207}\text{Pb}^*$	$\pm (\text{Ma})$	(Ma)	$\pm (\text{Ma})$	
RO295BF-26	71	25402	2.0	18.5914	12.8	0.7163	12.8	0.0966	0.7	0.05	594.3	4.0	548.5	54.3	362.2	289.3	594.3	4.0	164.1
RO295BF-27	30	1904	1.3	14.5848	12.7	0.9099	13.0	0.0963	2.7	0.21	592.4	15.1	657.0	62.7	885.7	263.0	592.4	15.1	66.9
RO295BF-28	75	9122	1.4	18.8548	11.0	0.6615	11.1	0.0905	1.6	0.14	558.2	8.6	515.5	44.8	330.4	249.5	558.2	8.6	169.0
RO295BF-29	394	70680	11.6	17.1157	4.9	0.7191	4.9	0.0893	0.9	0.18	551.2	4.8	550.2	21.0	545.8	106.1	551.2	4.8	101.0
RO295BF-30	142	15014	1.3	16.2075	5.1	0.7985	5.7	0.0939	2.4	0.42	578.3	13.2	596.0	25.5	663.7	109.8	578.3	13.2	87.1
RO295BF-31	200	50506	3.9	17.3937	4.0	0.7173	4.0	0.0905	0.5	0.12	558.5	2.7	549.1	17.0	510.5	87.6	558.5	2.7	109.4
RO295BF-32	80	21248	1.6	17.2276	9.7	0.7386	9.8	0.0923	1.5	0.15	569.0	8.0	561.6	42.3	531.5	212.8	569.0	8.0	107.1
RO295BF-33	82	11848	0.9	16.1553	5.6	0.7967	5.6	0.0934	0.8	0.14	575.3	4.3	595.0	25.3	670.6	119.3	575.3	4.3	85.8
RO295BF-34	106	38600	1.5	16.2008	8.4	0.7526	8.9	0.0884	2.8	0.32	546.2	14.8	569.7	38.7	664.6	180.4	546.2	14.8	82.2
RO295BF-35	117	41558	1.5	17.6244	8.0	0.6829	8.1	0.0873	1.3	0.16	539.5	6.7	528.5	33.5	481.4	177.6	539.5	6.7	112.1
RO295BF-36	104	32260	0.7	16.1102	5.7	0.7676	5.8	0.0897	1.2	0.20	553.7	6.1	578.4	25.7	676.6	122.0	553.7	6.1	81.8
RO295BF-37	62	18800	1.5	15.6882	14.1	0.7642	14.5	0.0870	3.3	0.23	537.5	17.0	576.5	63.7	733.1	299.8	537.5	17.0	73.3
RO295BF-37A	91	29302	1.2	16.9480	6.0	0.7160	6.1	0.0880	1.3	0.21	543.8	6.8	548.3	25.9	567.3	130.1	543.8	6.8	95.9
RO295BF-37B	105	27202	1.1	16.2576	6.0	0.7117	6.7	0.0839	2.8	0.42	519.5	13.9	545.8	28.1	657.1	129.8	519.5	13.9	79.1
RO295BF-38	57	13808	1.6	18.4970	12.1	0.6703	12.3	0.0899	2.2	0.18	555.1	11.6	520.9	50.0	373.7	272.6	555.1	11.6	148.6
RO295BF-39	56	24784	2.0	16.4399	4.7	0.7714	5.6	0.0920	3.0	0.53	567.2	16.0	580.5	24.7	633.2	102.1	567.2	16.0	89.6
RO295BF-40	84	7928	1.4	13.5236	18.1	0.9463	18.2	0.0928	1.4	0.08	572.2	7.8	676.2	89.8	1039.9	368.2	572.2	7.8	55.0
RO295BF-41	76	12114	1.5	16.5226	9.5	0.7571	10.0	0.0907	3.0	0.31	559.9	16.3	572.4	43.6	622.3	205.0	559.9	16.3	90.0
RO295BF-42	81	21128	1.8	17.6393	7.8	0.7115	8.3	0.0910	2.7	0.32	561.6	14.4	545.7	35.0	479.5	173.7	561.6	14.4	117.1
RO295BF-43	51	13152	1.5	17.4654	4.5	0.7450	4.6	0.0944	1.1	0.24	581.3	6.2	565.3	20.1	501.4	99.2	581.3	6.2	115.9
RO295BF-44	70	27856	1.6	15.5365	7.3	0.7946	7.7	0.0895	2.5	0.32	552.8	13.0	593.8	34.6	753.6	154.0	552.8	13.0	73.4
RO295BF-45	107	14194	1.7	17.4060	5.1	0.7421	5.3	0.0937	1.6	0.30	577.3	8.8	563.6	23.1	508.9	112.1	577.3	8.8	113.4
RO295BF-46	130	70362	1.3	16.7911	5.4	0.7558	5.6	0.0920	1.5	0.27	567.6	8.1	571.6	24.5	587.5	117.0	567.6	8.1	96.6

Annex 3

Isotopic data for sample 295, Struma diorite, near the village of Tsurvishte

Analysis	U (ppm)	Isotope ratios					error corr.	Apparent ages					Best age		Conc (%)				
		$^{206}\text{Pb}*/^{204}\text{Pb}$	U/Th	$^{206}\text{Pb}*/^{207}\text{Pb}^*$	$\pm (\%)$	$^{207}\text{Pb}*/^{235}\text{U}^*$	$\pm (\%)$	$^{206}\text{Pb}*/^{238}\text{U}$	$\pm (\%)$	$^{206}\text{Pb}*/^{238}\text{U}^*$	$\pm (\text{Ma})$	$^{207}\text{Pb}*/^{235}\text{U}$	$\pm (\text{Ma})$	$^{206}\text{Pb}*/^{207}\text{Pb}^*$	$\pm (\text{Ma})$	(Ma)	$\pm (\text{Ma})$		
RO-295-1	143	40588	3,9	17,5759	4,5	0,6750	5,0	0,0860	2,2	0,44	532,1	11,3	523,8	20,4	487,5	98,4	532,1	11,3	109,2
RO-295-2	679	218072	3,9	17,4507	2,6	0,6568	2,8	0,0831	1,1	0,37	514,8	5,2	512,7	11,3	503,3	57,5	514,8	5,2	102,3
RO-295-3	446	77456	3,2	17,7334	4,3	0,6540	4,4	0,0841	1,1	0,25	520,6	5,5	510,9	17,6	467,8	94,2	520,6	5,5	111,3
RO-295-4	204	70772	5,4	17,3138	5,0	0,6628	5,4	0,0832	2,2	0,41	515,4	11,0	516,3	22,0	520,6	109,0	515,4	11,0	99,0
RO-295-5	930	89048	2,5	17,4904	4,9	0,6391	4,9	0,0811	0,9	0,18	502,5	4,3	501,8	19,6	498,2	107,1	502,5	4,3	100,9
RO-295-6	579	41728	0,6	17,6468	3,5	0,6662	4,0	0,0853	1,8	0,47	527,5	9,3	518,4	16,1	478,6	77,4	527,5	9,3	110,2
RO-295-7	510	113738	4,6	17,0757	2,6	0,6712	2,7	0,0831	0,9	0,34	514,7	4,6	521,4	11,1	550,9	55,7	514,7	4,6	93,4
RO-295-8	107	23350	1,3	17,8548	8,4	0,6401	9,1	0,0829	3,4	0,37	513,4	16,7	502,4	36,1	452,6	187,9	513,4	16,7	113,4
RO-295-9	1392	280930	1,7	17,1206	4,0	0,6216	4,7	0,0772	2,5	0,52	479,3	11,4	490,8	18,4	545,2	88,1	479,3	11,4	87,9
RO-295-10	550	82138	3,6	16,8952	3,1	0,6757	3,2	0,0828	0,6	0,20	512,8	3,1	524,1	13,1	574,0	68,3	512,8	3,1	89,3
RO-295-11	365	37846	4,6	17,1250	4,0	0,6488	4,3	0,0806	1,5	0,35	499,6	7,2	507,8	17,2	544,6	88,1	499,6	7,2	91,7
RO-295-12	187	47160	4,1	17,6333	5,8	0,6501	5,8	0,0831	0,8	0,14	514,9	4,0	508,6	23,4	480,3	127,8	514,9	4,0	107,2
RO-295-13	251	31980	2,7	17,4991	5,1	0,6564	5,4	0,0833	1,8	0,33	515,8	8,9	512,4	21,9	497,2	113,1	515,8	8,9	103,8
RO-295-14	102	40836	1,6	18,4315	8,2	0,6716	8,4	0,0898	1,8	0,21	554,2	9,5	521,7	34,1	381,6	183,8	554,2	9,5	145,2
RO-295-15	153	38186	2,1	16,4839	3,7	0,7534	3,7	0,0901	0,7	0,18	556,0	3,5	570,2	16,3	627,4	79,0	556,0	3,5	88,6
RO-295-16	279	64608	4,8	17,4029	4,4	0,6964	4,8	0,0879	1,9	0,40	543,1	10,1	536,6	20,2	509,3	97,7	543,1	10,1	106,6
RO-295-17	90	28268	2,0	16,7812	11,3	0,7101	11,4	0,0864	1,4	0,13	534,3	7,3	544,8	47,9	588,7	245,1	534,3	7,3	90,8
RO-295-18	191	20358	2,0	16,8051	5,1	0,7449	5,1	0,0908	0,8	0,16	560,2	4,3	565,3	22,2	585,7	109,8	560,2	4,3	95,7
RO-295-19	276	34424	2,0	16,8462	5,6	0,7034	5,9	0,0859	1,6	0,27	531,5	8,1	540,8	24,6	580,4	122,7	531,5	8,1	91,6
RO-295-20	253	100260	2,2	16,6153	3,1	0,7855	3,5	0,0947	1,8	0,50	583,0	9,8	588,6	15,8	610,2	66,2	583,0	9,8	95,5
RO-295-22	419	81530	7,9	17,3299	2,4	0,6712	2,7	0,0844	1,3	0,48	522,1	6,4	521,4	11,0	518,5	51,9	522,1	6,4	100,7
RO-295-23	135	17554	2,4	16,1644	9,9	0,8100	9,9	0,0950	1,2	0,12	584,8	6,9	602,5	45,2	669,4	211,5	584,8	6,9	87,4
RO-295-24	94	15974	2,8	16,2240	16,5	0,6923	16,7	0,0815	3,0	0,18	504,9	14,5	534,2	69,6	661,5	354,8	504,9	14,5	76,3
RO-295-25	146	44374	1,9	17,5453	4,7	0,6755	5,8	0,0860	3,5	0,59	531,6	17,7	524,0	23,9	491,3	103,4	531,6	17,7	108,2
RO-295-26	182	26406	4,5	16,0405	30,9	0,7144	30,9	0,0831	0,9	0,03	514,7	4,6	547,4	131,5	685,9	674,3	514,7	4,6	75,0
RO-295-28	338	328242	2,0	16,6773	4,4	0,7193	4,5	0,0870	0,9	0,21	537,8	4,9	550,2	18,9	602,2	94,2	537,8	4,9	89,3
RO-295-29	197	43760	4,7	16,9164	5,5	0,6776	5,6	0,0831	1,1	0,19	514,8	5,2	525,4	22,9	571,3	119,5	514,8	5,2	90,1
RO-295-30	348	19334	3,9	17,2994	4,7	0,5964	5,5	0,0748	2,8	0,52	465,2	12,7	475,0	20,8	522,4	103,0	465,2	12,7	89,1

Annex 4

Isotope data for the zircons of sample 296 BF, granite dyke in Struma diorite, near the village of Tsurvishte

	U (ppm)	$^{206}\text{Pb}/^{204}\text{Pb}$	U/Th	$^{206}\text{Pb}^*/^{207}\text{Pb}^*$	± (%)	Isotope ratios			$^{206}\text{Pb}^*/^{238}\text{U}^*$	± (%)	Apparent ages			$^{206}\text{Pb}^*/^{207}\text{Pb}^*$	± (%)	Best age (Ma)	± (Ma)	Conc (%)	
						$^{207}\text{Pb}^*/^{235}\text{U}^*$	± (%)	$^{206}\text{Pb}^*/^{238}\text{U}$	± (%)	error corr.	$^{207}\text{Pb}^*/^{235}\text{U}$	± (Ma)	$^{206}\text{Pb}^*/^{238}\text{U}^*$	± (Ma)					
RO-296BF-1	264	34292	1,2	17,0342	3,7	0,7104	3,8	0,0878	1,0	0,27	542,3	5,3	545,0	16,1	556,2	80,2	542,3	5,3	97,5
RO-296BF-2	238	26390	1,2	16,7591	3,3	0,7023	3,4	0,0854	0,9	0,26	528,0	4,4	540,1	14,2	591,6	71,0	528,0	4,4	89,3
RO-296BF-3	404	2950	2,1	14,8988	2,7	0,8340	4,5	0,0901	3,6	0,79	556,2	19,0	615,8	20,7	841,5	56,8	556,2	19,0	66,1
RO-296BF-4	255	22468	2,9	17,0364	2,4	0,7263	3,9	0,0897	3,1	0,79	554,0	16,3	554,4	16,6	555,9	51,9	554,0	16,3	99,7
RO-296BF-5	140	14258	1,7	16,8787	8,3	0,7229	10,3	0,0885	6,1	0,59	546,7	32,0	552,4	43,9	576,1	180,5	546,7	32,0	94,9
RO-296BF-6	319	47230	2,5	16,9293	2,8	0,7320	3,0	0,0899	1,2	0,41	554,8	6,5	557,7	13,0	569,7	60,4	554,8	6,5	97,4
RO-296BF-7	83	12850	1,1	16,1319	6,7	0,7602	6,9	0,0889	1,6	0,24	549,3	8,5	574,1	30,1	673,8	142,6	549,3	8,5	81,5
RO-296BF-8	188	31646	4,1	16,9890	4,7	0,7618	4,8	0,0939	1,0	0,20	578,4	5,4	575,1	21,2	562,0	103,1	578,4	5,4	102,9
RO-296BF-9	255	17052	3,4	17,0550	2,5	0,7523	2,7	0,0931	1,0	0,36	573,6	5,3	569,5	11,9	553,5	55,5	573,6	5,3	103,6
RO-296BF-10	201	38284	2,2	16,9179	3,2	0,7549	3,5	0,0926	1,4	0,41	571,0	7,9	571,0	15,2	571,1	69,0	571,0	7,9	100,0
RO-296BF-11	356	31954	3,3	16,6824	2,6	0,7381	3,7	0,0893	2,7	0,72	551,4	14,3	561,3	16,2	601,5	56,1	551,4	14,3	91,7
RO-296BF-12	287	86176	1,9	16,5634	3,9	0,7636	4,0	0,0917	0,9	0,24	565,8	5,1	576,1	17,4	617,0	83,2	565,8	5,1	91,7
RO-296BF-13	119	19030	1,8	16,3933	3,4	0,7553	3,6	0,0898	1,1	0,32	554,4	6,1	571,3	15,6	639,3	72,5	554,4	6,1	86,7
RO-296BF-14	112	22906	1,3	16,6911	9,2	0,7268	9,3	0,0880	1,6	0,17	543,6	8,4	554,7	39,9	600,4	199,5	543,6	8,4	90,5
RO-296BF-15	184	15356	1,7	16,9161	3,4	0,7581	3,7	0,0930	1,4	0,39	573,3	7,9	572,9	16,0	571,4	73,1	573,3	7,9	100,3
RO-296BF-16	322	70284	1,8	16,8523	2,1	0,7648	2,2	0,0935	0,6	0,26	576,1	3,1	576,8	9,7	579,6	46,0	576,1	3,1	99,4
RO-296BF-17	443	48494	1,8	16,6610	3,4	0,7473	3,4	0,0903	0,6	0,18	557,3	3,3	566,7	15,0	604,3	73,4	557,3	3,3	92,2
RO-296BF-18	382	1358	1,0	12,9368	6,3	0,9842	7,2	0,0923	3,4	0,47	569,4	18,5	695,8	36,1	1128,9	125,9	569,4	18,5	50,4
RO-296BF-19	305	67766	2,9	17,1750	3,6	0,7131	3,8	0,0888	1,3	0,33	548,6	6,7	546,6	16,2	538,2	79,3	548,6	6,7	101,9
RO-296BF-20	397	1540	1,3	13,4723	10,7	0,9077	10,7	0,0887	0,9	0,08	547,8	4,7	655,9	51,8	1047,6	215,9	547,8	4,7	52,3
RO-296BF-21	391	37606	2,2	16,7788	1,7	0,7588	2,5	0,0923	1,8	0,73	569,4	10,0	573,3	11,1	589,1	37,6	569,4	10,0	96,7
RO-296BF-22	191	23548	2,5	17,3637	5,4	0,6993	5,5	0,0881	0,8	0,15	544,1	4,2	538,4	22,9	514,2	119,2	544,1	4,2	105,8
RO-296BF-23	298	23362	3,4	17,1477	2,9	0,7143	3,4	0,0888	1,8	0,53	548,7	9,4	547,3	14,3	541,7	62,6	548,7	9,4	101,3
RO-296BF-24	104	8700	0,9	16,4656	9,1	0,7476	9,1	0,0893	0,8	0,09	551,3	4,4	566,8	39,7	629,8	196,5	551,3	4,4	87,5
RO-296BF-25	249	18764	2,0	17,3944	3,0	0,7039	3,4	0,0888	1,6	0,47	548,5	8,5	541,1	14,3	510,4	66,1	548,5	8,5	107,5
RO-296BF-27	229	45534	2,1	16,4769	2,8	0,7467	2,9	0,0892	0,9	0,29	551,0	4,5	566,3	12,6	628,3	59,6	551,0	4,5	87,7

Annex 5

Isotopic data for sample 307, metagranite, road cuttings between the villages of Ribnik and Lebnitsa, Ograzhdenian supercomplex, Ograzhden Mts.

Analysis	U (ppm)	$^{206}\text{Pb}/^{204}\text{Pb}$	U/Th	$^{206}\text{Pb}^*/^{207}\text{Pb}^*$	$\pm(\%)$	Isotope ratios					$^{206}\text{Pb}^*/^{238}\text{U}^*$	$\pm(\text{Ma})$	Apparent ages				Best age (Ma)	$\pm(\text{Ma})$	Conc (%)
						$^{207}\text{Pb}^*/^{235}\text{U}^*$	$\pm(\%)$	$^{206}\text{Pb}^*/^{238}\text{U}$	$\pm(\%)$	error corr.			$^{207}\text{Pb}^*/^{235}\text{U}$	$\pm(\text{Ma})$	$^{206}\text{Pb}^*/^{207}\text{Pb}^*$	$\pm(\text{Ma})$			
RO-307BR-1	620	187640	234.8	17.9409	1.9	0.5731	2.3	0.0746	1.3	0.55	463.6	5.6	460.0	8.4	441.9	41.8	463.6	5.6	104.9
RO-307BR-2	60	85068	2.6	7.9978	2.5	6.0336	2.9	0.3500	1.4	0.48	1934.5	23.1	1980.7	25.0	2029.3	44.4	2029.3	44.4	95.3
RO-307BR-3	154	7328	3.8	16.0616	14.8	0.6318	17.0	0.0736	8.4	0.49	457.8	37.2	497.2	67.1	683.0	318.0	457.8	37.2	67.0
RO-307BR-4	262	23304	4.3	18.0136	3.2	0.5696	4.3	0.0744	2.8	0.65	462.7	12.3	457.7	15.7	432.9	72.2	462.7	12.3	106.9
RO-307BR-5	281	17448	20.7	17.4969	3.6	0.6205	3.7	0.0787	0.5	0.14	488.6	2.4	490.2	14.3	497.4	80.1	488.6	2.4	98.2
RO-307BR-7	212	28708	4.1	18.2750	3.4	0.5625	3.8	0.0746	1.7	0.44	463.5	7.4	453.1	13.7	400.8	75.5	463.5	7.4	115.7
RO-307BR-8	235	23654	2.4	17.4439	4.9	0.5821	5.0	0.0736	0.7	0.13	458.1	2.9	465.8	18.5	504.1	108.1	458.1	2.9	90.9
RO-307BR-9	319	29108	14.6	17.7686	4.3	0.5668	4.5	0.0730	1.0	0.22	454.5	4.4	456.0	16.4	463.4	96.4	454.5	4.4	98.1
RO-307BR-10	158	28062	6.5	15.6187	3.3	0.9864	5.7	0.1117	4.7	0.82	682.8	30.1	696.9	28.7	742.5	69.7	682.8	30.1	92.0
RO-307BR-12	1718	453274	26.9	17.8555	1.6	0.5920	1.8	0.0767	0.9	0.49	476.2	4.0	472.1	6.7	452.5	34.4	476.2	4.0	105.2
RO-307BR-13	239	14214	4.7	18.1202	3.5	0.5188	4.3	0.0682	2.5	0.58	425.2	10.3	424.4	15.0	419.8	78.9	425.2	10.3	101.3
RO-307BR-14	489	51010	2.3	16.9173	1.9	0.7554	2.2	0.0927	1.0	0.48	571.4	5.7	571.3	9.5	571.2	41.6	571.4	5.7	100.0
RO-307BR-15	258	17802	11.1	16.8663	3.2	0.6352	3.5	0.0777	1.4	0.39	482.4	6.3	499.3	13.8	577.7	70.0	482.4	6.3	83.5
RO-307BR-16	96	25522	2.5	16.9540	7.0	0.7448	7.6	0.0916	3.1	0.40	564.9	16.7	565.2	33.0	566.5	151.6	564.9	16.7	99.7
RO-307BR-18	193	135362	2.7	7.0403	2.3	7.0010	5.4	0.3575	4.9	0.91	1970.2	83.7	2111.6	48.2	2252.2	38.9	2252.2	38.9	87.5
RO-307BR-20	439	54288	1.7	16.6336	2.1	0.6565	2.2	0.0792	0.8	0.34	491.3	3.6	512.4	8.9	607.8	44.8	491.3	3.6	80.8
RO-307BR-22	297	57476	4.7	15.9962	2.6	0.7857	3.2	0.0912	1.9	0.59	562.4	10.1	588.7	14.3	691.8	55.1	562.4	10.1	81.3
RO-307BR-23	480	99292	9.7	15.1984	2.5	0.9774	3.4	0.1077	2.3	0.68	659.6	14.4	692.3	16.9	799.9	52.0	659.6	14.4	82.5
RO-307BR-24	194	24336	8.9	17.7086	7.4	0.5790	8.0	0.0744	3.1	0.38	462.4	13.6	463.8	29.8	470.9	163.9	462.4	13.6	98.2
RO-307BR-25	637	62230	4.2	15.9494	2.2	0.9179	3.2	0.1062	2.4	0.74	650.5	14.7	661.2	15.6	698.0	46.2	650.5	14.7	93.2
RO-307BR-26	185	26620	7.2	17.0679	4.8	0.5826	5.0	0.0721	1.4	0.28	448.9	6.1	466.1	18.7	551.9	104.7	448.9	6.1	81.3
RO-307BR-27	563	66008	1.3	16.6002	2.2	0.8590	3.6	0.1034	2.8	0.79	634.4	17.0	629.6	16.8	612.2	47.6	634.4	17.0	103.6
RO-307BR-28	408	94534	2.7	16.5973	3.5	0.7664	3.9	0.0923	1.6	0.41	568.9	8.6	577.7	17.0	612.6	76.1	568.9	8.6	92.9
RO-307BR-29	280	18408	1.9	17.1614	5.6	0.6027	5.9	0.0750	1.8	0.30	466.3	7.9	478.9	22.5	540.0	122.9	466.3	7.9	86.4
RO-307BR-30	404	47642	1.3	16.4048	2.1	0.8216	3.1	0.0977	2.2	0.72	601.2	12.6	608.9	14.0	637.8	45.9	601.2	12.6	94.3
RO-307BR-31	362	17926	7.9	17.4941	4.6	0.5467	5.5	0.0694	3.1	0.55	432.4	12.8	442.9	19.9	497.8	101.5	432.4	12.8	86.9
RO-307BR-32	254	27884	9.1	18.1427	4.3	0.5675	4.4	0.0747	0.9	0.21	464.3	4.2	456.4	16.0	417.0	95.1	464.3	4.2	111.3
RO-307BR-33	280	28382	3.5	17.9493	3.5	0.5372	4.2	0.0699	2.3	0.55	435.7	9.9	436.5	15.0	440.9	78.3	435.7	9.9	98.8
RO-307BR-34	318	98396	3.8	8.6654	0.9	4.0969	1.2	0.2575	0.9	0.69	1476.9	11.4	1653.7	10.1	1886.2	16.0	1886.2	16.0	78.3
RO-307BR-35	241	361004	7.7	5.9965	1.6	10.7512	2.1	0.4676	1.4	0.67	2472.9	29.4	2501.9	19.9	2525.4	26.7	2525.4	26.7	97.9
RO-307BR-36	164	23712	6.7	16.4907	3.7	0.7713	4.9	0.0922	3.1	0.65	568.8	17.1	580.5	21.5	626.5	79.8	568.8	17.1	90.8
RO-307BR-38	396	48946	1.3	16.4592	2.2	0.8019	2.4	0.0957	1.0	0.41	589.3	5.5	597.9	10.7	630.6	46.4	589.3	5.5	93.5
RO-307BR-39	374	42420	1.9	16.6050	2.3	0.7919	2.5	0.0954	1.1	0.45	587.2	6.4	592.2	11.4	611.6	48.9	587.2	6.4	96.0
RO-307BR-40	765	133212	1.5	15.7404	130	1.0231	1.5	0.1168	0.9	0.63	712.1	6.2	715.4	7.4	726.0	23.8	712.1	6.2	98.1

Annex 6

Isotopic data for sample 306, biotite migmatites hosting the Ribnik metagranite, road cuttings near the village of Ribnik, Ograzhdenian supercomplex, Ograzhden Mts.

	U (ppm)	$^{206}\text{Pb}/^{204}\text{Pb}$	U/Th	$^{206}\text{Pb}^*/^{207}\text{Pb}^*$ ± (%)	Isotope ratios					Apparent ages					Best age (Ma)	±(Ma)	Conc (%)		
					$^{207}\text{Pb}^*/^{235}\text{U}^*$	±(%)	$^{206}\text{Pb}^*/^{238}\text{U}$	±(%)	error corr.	$^{206}\text{Pb}^*/^{238}\text{U}^*$	±(Ma)	$^{207}\text{Pb}^*/^{235}\text{U}$	±(Ma)	$^{206}\text{Pb}^*/^{207}\text{Pb}^*$	±(Ma)				
RO-306BR-1	200	6338	2.2	17.9236	5.1	0.5525	5.2	0.0718	1.0	0.19	447.1	4.3	446.7	18.6	444.1	112.5	447.1	4.3	100.7
RO-306BR-2	190	7492	5.1	18.1840	2.7	0.5691	2.8	0.0751	0.8	0.28	466.6	3.5	457.5	10.4	411.9	60.6	466.6	3.5	113.3
RO-306BR-3	333	11470	3.3	17.9923	3.0	0.5366	3.1	0.0700	1.0	0.31	436.3	4.1	436.2	11.1	435.6	66.6	436.3	4.1	100.2
RO-306BR-4	369	12088	6.1	18.1066	3.3	0.5677	4.0	0.0746	2.3	0.56	463.5	10.1	456.5	14.7	421.5	73.9	463.5	10.1	110.0
RO-306BR-5	165	4952	3.6	18.2893	4.4	0.5428	4.4	0.0720	0.7	0.16	448.2	3.1	440.3	15.8	399.0	97.9	448.2	3.1	112.3
RO-306BR-6	304	9394	2.4	18.3565	2.9	0.5187	3.3	0.0691	1.5	0.47	430.5	6.4	424.3	11.3	390.8	64.7	430.5	6.4	110.2
RO-306BR-7	232	9888	8.9	17.4468	4.5	0.5558	4.6	0.0703	1.1	0.24	438.1	4.6	448.8	16.8	503.7	98.9	438.1	4.6	87.0
RO-306BR-8	95	2318	9.4	16.8161	6.4	0.5262	6.5	0.0642	1.2	0.18	400.9	4.5	429.3	22.9	584.2	140.0	400.9	4.5	68.6
RO-306BR-9	340	14412	5.0	16.8439	2.5	0.6511	3.3	0.0795	2.2	0.67	493.3	10.5	509.1	13.2	580.6	53.5	493.3	10.5	85.0
RO-306BR-10	286	12538	10.2	17.9978	3.3	0.5238	4.0	0.0684	2.1	0.54	426.3	8.8	427.7	13.8	434.9	74.2	426.3	8.8	98.0
RO-306BR-11	267	5414	1.9	17.4755	6.9	0.5424	7.6	0.0687	3.2	0.42	428.6	13.3	440.0	27.2	500.2	152.1	428.6	13.3	85.7
RO-306BR-12	178	9300	3.1	18.0496	5.6	0.5476	5.8	0.0717	1.4	0.23	446.3	5.9	443.4	20.9	428.5	125.9	446.3	5.9	104.2
RO-306BR-13	504	8072	3.0	17.0039	2.2	0.5356	3.5	0.0661	2.7	0.78	412.3	10.9	435.5	12.4	560.1	47.6	412.3	10.9	73.6
RO-306BR-14	171	6892	3.0	19.1412	7.6	0.5140	7.6	0.0714	0.9	0.11	444.3	3.7	421.1	26.3	296.1	173.3	444.3	3.7	150.1
RO-306BR-15	354	10652	2.7	18.1349	3.5	0.5252	4.4	0.0691	2.6	0.59	430.6	10.8	428.6	15.2	418.0	78.3	430.6	10.8	103.0
RO-306BR-16	427	8988	3.8	17.6353	3.0	0.5621	3.1	0.0719	1.0	0.30	447.5	4.1	452.9	11.4	480.0	65.9	447.5	4.1	93.2
RO-306BR-17	181	8190	1.1	17.9905	5.5	0.5502	5.9	0.0718	2.0	0.34	446.9	8.8	445.1	21.3	435.8	123.6	446.9	8.8	102.6
RO-306BR-18	1291	33472	2.3	17.9124	1.3	0.5539	3.3	0.0720	3.0	0.91	448.0	12.9	447.6	11.8	445.5	29.9	448.0	12.9	100.6
RO-306BR-19	444	14844	7.5	17.8784	1.6	0.5473	1.8	0.0710	0.7	0.39	441.9	2.9	443.2	6.3	449.7	35.9	441.9	2.9	98.3
RO-306BR-20	268	5162	4.8	17.1510	3.3	0.5511	3.4	0.0685	0.9	0.26	427.4	3.6	445.7	12.3	541.3	71.8	427.4	3.6	79.0
RO-306BR-21	232	7508	9.1	17.9900	6.0	0.5298	6.0	0.0691	0.5	0.08	430.9	2.1	431.7	21.2	435.9	134.1	430.9	2.1	98.9
RO-306BR-22	206	9330	1.4	14.1356	2.8	1.3650	2.9	0.1399	0.6	0.19	844.4	4.4	874.0	16.8	950.0	57.7	844.4	4.4	88.9
RO-306BR-23	1674	80580	21.0	17.5644	1.3	0.5988	2.5	0.0763	2.2	0.85	473.9	9.9	476.5	9.7	489.0	29.6	473.9	9.9	96.9
RO-306BR-24	416	37264	4.5	14.8829	1.7	1.1846	2.1	0.1279	1.4	0.63	775.7	9.9	793.4	11.8	843.7	34.6	775.7	9.9	91.9
RO-306BR-25	140	5800	5.8	17.7505	6.7	0.5463	6.8	0.0703	1.2	0.17	438.1	4.9	442.6	24.3	465.7	148.3	438.1	4.9	94.1
RO-306BR-26	266	10798	7.1	18.1641	2.8	0.5375	3.5	0.0708	2.1	0.60	441.0	9.0	436.8	12.3	414.4	61.9	441.0	9.0	106.4
RO-306BR-27	124	6454	2.6	18.7517	6.9	0.5454	6.9	0.0742	1.1	0.15	461.2	4.7	442.0	24.9	342.8	155.6	461.2	4.7	134.5
RO-306BR-28	380	17720	5.4	16.9946	2.0	0.6334	2.3	0.0781	1.2	0.51	484.6	5.6	498.2	9.1	561.3	43.3	484.6	5.6	86.3
RO-306BR-29	345	14672	23.6	17.2038	2.9	0.6289	2.9	0.0785	0.5	0.17	487.0	2.3	495.4	11.5	534.6	63.1	487.0	2.3	91.1
RO-306BR-30	296	12816	1.5	18.1288	4.1	0.5406	4.3	0.0711	1.1	0.27	442.6	4.9	438.8	15.2	418.7	92.1	442.6	4.9	105.7
RO-306BR-31	192	9804	4.6	18.1526	4.8	0.5451	4.9	0.0718	0.9	0.18	446.8	3.9	441.8	17.4	415.8	106.9	446.8	3.9	107.4

Annex 7

Isotopic data for sample 304, biotite migmatites, road cuttings between the villages of Mikrevo and Tsaparevo

Zircons	U (ppm)	$^{206}\text{Pb}/^{204}\text{Pb}$	U/Th	$^{206}\text{Pb}^*/^{207}\text{Pb}^*$	$\pm(\%)$	Isotope ratios					Apparent ages					Best age (Ma)	$\pm(\text{Ma})$	Conc (%)	
						$^{207}\text{Pb}^*/^{235}\text{U}^*$	$\pm(\%)$	$^{206}\text{Pb}^*/^{238}\text{U}$	$\pm(\%)$	error corr.	$^{206}\text{Pb}^*/^{238}\text{U}^*$	$\pm(\text{Ma})$	$^{207}\text{Pb}^*/^{235}\text{U}$	$\pm(\text{Ma})$	$^{206}\text{Pb}^*/^{207}\text{Pb}^*$	$\pm(\text{Ma})$			
RO-304BGN-1	262	48752	3,5	17,7760	3,4	0,5934	3,7	0,0765	1,3	0,36	475,2	6,0	473,1	13,9	462,5	76,0	475,2	6,0	102,8
RO-304BGN-2	1304	106882	2,9	16,3300	2,9	0,8445	3,9	0,1000	2,7	0,69	614,5	15,9	621,6	18,3	647,6	61,5	614,5	15,9	94,9
RO-304BGN-3	720	167648	2,6	17,9969	1,6	0,5701	2,5	0,0744	1,9	0,77	462,7	8,7	458,1	9,3	435,0	35,9	462,7	8,7	106,4
RO-304BGN-4	1252	63946	22,6	17,7581	2,1	0,5488	2,2	0,0707	0,8	0,34	440,3	3,2	444,2	8,0	464,7	46,4	440,3	3,2	94,7
RO-304BGN-5	454	102232	8,5	17,6089	3,5	0,5897	3,6	0,0753	0,9	0,26	468,1	4,2	470,7	13,5	483,4	76,7	468,1	4,2	96,8
RO-304BGN-6	456	59314	8,1	18,1019	4,7	0,5660	4,7	0,0743	0,6	0,13	462,1	2,8	455,4	17,2	422,0	103,9	462,1	2,8	109,5
RO-304BGN-8	1627	149046	165,7	18,5344	1,8	0,4149	2,4	0,0558	1,7	0,69	349,9	5,7	352,4	7,2	369,1	39,7	349,9	5,7	94,8
RO-304BGN-9	486	130580	2,4	17,9761	3,8	0,5565	3,8	0,0725	0,7	0,17	451,5	2,8	449,2	14,0	437,6	84,4	451,5	2,8	103,2
RO-304BGN-10	416	432610	12,1	8,4263	3,2	3,8302	3,9	0,2341	2,3	0,58	1355,8	27,6	1599,1	31,2	1936,4	56,4	1936,4	56,4	70,0
RO-304BGN-11	614	146964	13,0	17,9763	3,0	0,5466	3,4	0,0713	1,7	0,48	443,8	7,1	442,8	12,3	437,6	67,1	443,8	7,1	101,4
RO-304BGN-12	190	29456	12,1	17,0721	4,8	0,5522	6,2	0,0684	3,9	0,63	426,4	16,2	446,5	22,4	551,3	105,3	426,4	16,2	77,3
RO-304BGN-13	490	87990	12,7	17,9089	2,3	0,5764	2,6	0,0749	1,2	0,46	465,5	5,5	462,2	9,8	445,9	52,1	465,5	5,5	104,4
RO-304BGN-14	497	123246	4,0	14,2625	2,7	1,5223	2,8	0,1575	0,7	0,26	942,7	6,3	939,4	17,0	931,7	55,0	942,7	6,3	101,2
RO-304BGN-17	248	21196	6,8	17,9247	6,1	0,5514	6,8	0,0717	2,9	0,43	446,3	12,6	445,9	24,5	444,0	136,1	446,3	12,6	100,5
RO-304BGN-18	544	83002	6,1	17,4152	3,4	0,5656	3,7	0,0714	1,3	0,35	444,8	5,5	455,2	13,4	507,8	75,2	444,8	5,5	87,6
RO-304BGN-19	558	86830	28,3	18,1713	2,4	0,4682	3,1	0,0617	1,9	0,63	386,0	7,2	390,0	9,9	413,5	53,3	386,0	7,2	93,4
RO-304BGN-20	172	31096	7,2	18,3791	8,3	0,5803	8,6	0,0774	2,1	0,24	480,3	9,7	464,7	32,0	388,0	187,1	480,3	9,7	123,8
RO-304BGN-21	264	75300	6,3	17,6498	6,8	0,6095	8,8	0,0780	5,6	0,64	484,3	26,2	483,2	33,8	478,2	149,6	484,3	26,2	101,3
RO-304BGN-24	259	37098	4,4	17,5420	3,9	0,6208	4,2	0,0790	1,5	0,36	490,0	7,1	490,3	16,4	491,8	87,0	490,0	7,1	99,6
RO-304BGN-25	349	88568	11,4	17,6453	3,7	0,5540	3,9	0,0709	1,1	0,28	441,6	4,7	447,6	14,0	478,8	82,1	441,6	4,7	92,2
RO-304BGN-26	269	27272	7,9	16,5148	6,0	0,5836	7,7	0,0699	4,8	0,62	435,6	20,3	466,8	28,9	623,3	130,0	435,6	20,3	69,9
RO-304BGN-27	323	21898	2,6	16,9915	5,5	0,5668	5,5	0,0699	0,8	0,14	435,3	3,2	456,0	20,3	561,6	119,1	435,3	3,2	77,5

Zircons	U (ppm)	$^{206}\text{Pb}/^{204}\text{Pb}$	U/Th	$^{206}\text{Pb}^*/^{207}\text{Pb}^*$		$\pm(\%)$	Isotope ratios					Apparent ages					Best age (Ma)	$\pm(\text{Ma})$	Conc (%)
				$^{207}\text{Pb}^*/^{235}\text{U}^*$	$\pm(\%)$		$^{206}\text{Pb}^*/^{238}\text{U}$	$\pm(\%)$	error corr.	$^{206}\text{Pb}^*/^{238}\text{U}^*$	$\pm(\text{Ma})$	$^{207}\text{Pb}^*/_{235}\text{U}$	$\pm(\text{Ma})$	$^{206}\text{Pb}^*/^{207}\text{Pb}^*$	$\pm(\text{Ma})$				
RO-304BGN-28	455	45190	1,8	17,9220	1,0	0,5429	1,4	0,0706	1,0	0,69	439,6	4,1	440,4	5,0	444,3	22,6	439,6	4,1	98,9
RO-304BGN-29	281	41340	8,5	17,6827	4,1	0,5702	4,3	0,0731	1,3	0,31	455,0	5,9	458,1	15,8	474,1	89,9	455,0	5,9	96,0
RO-304BGN-30	313	64964	12,3	16,5794	4,8	0,6068	5,2	0,0730	2,0	0,38	454,0	8,6	481,5	20,0	614,9	104,2	454,0	8,6	73,8
RO-304BGN-31	475	83744	76,8	17,2917	5,2	0,5599	5,7	0,0702	2,4	0,41	437,5	9,9	451,5	20,8	523,3	114,2	437,5	9,9	83,6
RO-304BGN-32	587	282816	8,1	16,5416	4,7	0,8108	4,8	0,0973	0,9	0,20	598,4	5,3	602,9	21,6	619,8	100,6	598,4	5,3	96,5
RO-304BGN-33	244	8366	9,1	16,2669	10,6	0,6099	10,6	0,0720	0,5	0,05	447,9	2,3	483,5	40,9	655,9	228,0	447,9	2,3	68,3
RO-304BGN-34	201	33676	4,3	17,5521	6,0	0,5402	7,8	0,0688	4,9	0,63	428,8	20,2	438,6	27,7	490,5	133,3	428,8	20,2	87,4
RO-304BGN-35	192	90308	3,9	18,7960	8,2	0,5118	8,6	0,0698	2,5	0,29	434,8	10,3	419,7	29,5	337,5	186,3	434,8	10,3	128,8
RO-304BGN-36	189	34846	7,6	17,7245	6,4	0,5706	6,8	0,0734	2,3	0,34	456,3	10,3	458,4	25,0	468,9	140,8	456,3	10,3	97,3
RO-304BGN-38	175	35240	5,7	17,1410	6,9	0,5822	6,9	0,0724	0,8	0,11	450,5	3,4	465,9	25,8	542,5	150,3	450,5	3,4	83,0
RO-304BGN-39	585	275372	27,0	17,6925	4,4	0,5486	5,1	0,0704	2,7	0,52	438,5	11,2	444,1	18,5	472,9	97,4	438,5	11,2	92,7
RO-304BGN-40	283	34752	12,5	17,5377	7,7	0,6209	9,7	0,0790	5,9	0,61	490,0	27,9	490,4	37,7	492,3	169,6	490,0	27,9	99,5
RO-304BGN-41	484	185946	4,6	14,6706	3,0	1,3223	3,7	0,1407	2,1	0,57	848,6	16,7	855,5	21,2	873,5	62,1	848,6	16,7	97,1
RO-304BGN-42	319	283190	13,2	18,1710	3,1	0,5525	3,2	0,0728	1,0	0,31	453,1	4,4	446,6	11,7	413,5	69,1	453,1	4,4	109,6
RO-304BGN-43	134	29992	2,1	18,8451	8,7	0,5500	8,8	0,0752	1,1	0,12	467,2	4,9	445,0	31,8	331,6	198,7	467,2	4,9	140,9
RO-304BGN-44	327	47432	13,2	18,1681	3,4	0,5352	4,0	0,0705	2,2	0,54	439,3	9,2	435,2	14,1	413,9	75,0	439,3	9,2	106,1
RO-304BGN-45	240	37510	13,0	17,5126	5,9	0,5407	7,3	0,0687	4,4	0,60	428,1	18,1	438,9	26,2	495,5	129,9	428,1	18,1	86,4
RO-304BGN-46	848	284770	26,1	17,0862	4,2	0,5969	5,7	0,0740	3,8	0,68	460,0	17,0	475,3	21,5	549,5	91,1	460,0	17,0	83,7
RO-304BGN-48	181	39000	3,3	17,8728	7,3	0,5562	7,3	0,0721	1,1	0,15	448,8	4,6	449,0	26,7	450,4	161,5	448,8	4,6	99,6
RO-304BGN-49	248	131390	9,5	17,7736	4,2	0,5686	4,3	0,0733	1,1	0,24	456,0	4,7	457,1	16,0	462,8	93,4	456,0	4,7	98,5
RO-304BGN-50	81	16312	2,8	16,8724	14,6	0,5761	14,9	0,0705	3,2	0,21	439,1	13,4	461,9	55,3	577,0	318,0	439,1	13,4	76,1
RO-304BGN-51	228	34744	1,9	18,1197	6,8	0,5472	7,0	0,0719	1,5	0,22	447,7	6,5	443,2	25,1	419,8	152,6	447,7	6,5	106,6
RO-304BGN-52	525	127318	2,4	18,3897	4,5	0,5388	6,3	0,0719	4,5	0,70	447,4	19,2	437,6	22,5	386,7	100,9	447,4	19,2	115,7

Annex 8

Isotopic data for zircons from sample 302, biotite migmatite, near the tunnel south of Yavorov Railway Station

Analysis	U (ppm)	Isotope ratios						Error corr.	$^{206}\text{Pb}^*/^{238}\text{U}^*$	$\pm(\text{Ma})$	Apparent ages			Best age (Ma)	$\pm(\text{Ma})$	Conc (%)			
		$^{206}\text{Pb}^*/^{204}\text{Pb}$	U/Th	$^{206}\text{Pb}^*/^{207}\text{Pb}^*$	$\pm(\%)$	$^{207}\text{Pb}^*/^{235}\text{U}^*$	$\pm(\%)$				$^{207}\text{Pb}^*/^{235}\text{U}$	$\pm(\text{Ma})$	$^{206}\text{Pb}^*/^{207}\text{Pb}^*$	$\pm(\text{Ma})$					
RO-302BO-1	609	26252	2,8	17,5663	2,3	0,5938	4,5	0,0757	3,9	0,86	470,1	17,7	473,3	17,2	488,7	51,1	470,1	17,7	96,2
RO-302BO-2	410	23038	3,4	18,1448	2,9	0,5361	3,2	0,0706	1,4	0,43	439,5	5,9	435,9	11,4	416,8	65,3	439,5	5,9	105,5
RO-302BO-3	464	15868	3,6	17,5826	2,4	0,5715	3,1	0,0729	2,0	0,65	453,5	8,9	459,0	11,5	486,7	52,3	453,5	8,9	93,2
RO-302BO-4	788	32784	3,3	17,8734	2,1	0,5698	2,5	0,0739	1,4	0,55	459,4	6,2	457,9	9,3	450,3	46,6	459,4	6,2	102,0
RO-302BO-5	520	27246	2,1	17,7540	2,4	0,5759	4,1	0,0742	3,3	0,81	461,1	14,7	461,8	15,1	465,2	52,7	461,1	14,7	99,1
RO-302BO-6	48	2318	247,4	22,2791	26,7	0,3355	26,8	0,0542	1,2	0,05	340,3	4,0	293,8	68,4	-61,9	662,1	340,3	4,0	-550,1
RO-302BO-7	138	6630	3,4	18,5528	4,5	0,5108	4,6	0,0687	0,6	0,13	428,5	2,4	419,0	15,7	366,9	102,2	428,5	2,4	116,8
RO-302BO-8	183	12824	3,5	17,9765	3,7	0,5698	3,9	0,0743	1,4	0,36	462,0	6,2	457,9	14,5	437,5	81,7	462,0	6,2	105,6
RO-302BO-9	183	9456	3,1	17,5212	7,2	0,6059	7,3	0,0770	1,4	0,19	478,2	6,3	481,0	28,0	494,4	158,6	478,2	6,3	96,7
RO-302BO-10	492	33730	2,2	17,8270	2,7	0,5984	3,2	0,0774	1,7	0,54	480,4	8,0	476,2	12,3	456,1	60,4	480,4	8,0	105,3
RO-302BO-11	492	19722	1,8	17,7465	2,8	0,5740	3,1	0,0739	1,3	0,43	459,5	5,9	460,6	11,5	466,2	61,9	459,5	5,9	98,6
RO-302BO-12	289	14012	3,4	17,8954	2,5	0,5429	2,8	0,0705	1,2	0,44	438,9	5,3	440,3	10,1	447,6	56,6	438,9	5,3	98,1
RO-302BO-13	428	18314	2,0	16,9280	6,2	0,6331	7,0	0,0777	3,3	0,46	482,5	15,1	498,0	27,6	569,8	135,4	482,5	15,1	84,7
RO-302BO-14	831	19582	611,4	18,5221	2,8	0,3791	3,7	0,0509	2,5	0,68	320,2	7,9	326,4	10,5	370,6	62,1	320,2	7,9	86,4
RO-302BO-15	728	44446	1,4	17,5825	2,4	0,5777	2,9	0,0737	1,6	0,56	458,2	7,1	463,0	10,6	486,7	52,4	458,2	7,1	94,1
RO-302BO-16	266	5074	2,5	16,4807	4,6	0,6101	4,7	0,0729	0,6	0,13	453,7	2,7	483,6	18,0	627,8	100,2	453,7	2,7	72,3
RO-302BO-17	284	8934	2,2	17,3985	3,2	0,5629	4,6	0,0710	3,3	0,73	442,4	14,3	453,4	16,8	509,9	69,4	442,4	14,3	86,8
RO-302BO-18	21	868	79,6	36,2784	92,6	0,1804	92,7	0,0475	4,4	0,05	298,9	12,8	168,4	144,8	-1427,1	1897,9	298,9	12,8	-20,9
RO-302BO-19	710	11942	1,7	17,3133	5,6	0,5366	5,7	0,0674	1,4	0,25	420,3	5,8	436,2	20,3	520,6	122,0	420,3	5,8	80,7
RO-302BO-20	250	16466	2,9	17,8520	2,7	0,5691	4,4	0,0737	3,5	0,80	458,3	15,6	457,4	16,3	453,0	59,5	458,3	15,6	101,2
RO-302BO-21	664	26338	2,2	17,6806	1,8	0,5727	2,4	0,0734	1,7	0,68	456,8	7,3	459,7	9,0	474,4	39,2	456,8	7,3	96,3
RO-302BO-22	635	18232	1,5	17,4012	1,5	0,5941	2,1	0,0750	1,5	0,69	466,1	6,7	473,5	8,1	509,5	33,7	466,1	6,7	91,5
RO-302BO-23	356	14494	1,9	16,4197	6,4	0,7479	6,5	0,0891	1,1	0,17	550,0	6,0	567,0	28,1	635,8	137,0	550,0	6,0	86,5
RO-302BO-24	501	20686	2,1	17,7298	1,7	0,5984	2,8	0,0769	2,2	0,79	477,8	10,3	476,2	10,7	468,2	38,2	477,8	10,3	102,1
RO-302BO-25	227	10846	2,5	17,9486	5,8	0,5899	6,0	0,0768	1,3	0,21	476,9	5,8	470,8	22,4	441,0	129,4	476,9	5,8	108,2
RO-302BO-26	280	14880	2,2	17,6930	2,5	0,6185	3,2	0,0794	2,0	0,63	492,4	9,4	488,9	12,3	472,8	54,5	492,4	9,4	104,1
RO-302BO-27	360	17490	2,1	17,9734	3,7	0,6055	3,8	0,0789	1,1	0,27	489,8	5,0	480,7	14,6	437,9	81,8	489,8	5,0	111,8
RO-302BO-28	329	19102	2,7	17,6829	2,2	0,6151	2,6	0,0789	1,3	0,49	489,5	5,9	486,8	10,0	474,1	49,8	489,5	5,9	103,2
RO-302BO-29	335	13934	3,1	17,6839	3,3	0,5759	3,8	0,0739	1,9	0,49	459,4	8,2	461,8	14,1	474,0	73,0	459,4	8,2	96,9
RO-302BO-30	260	17316	2,7	17,9637	2,7	0,6017	3,4	0,0784	2,1	0,60	486,5	9,7	478,3	13,0	439,1	60,7	486,5	9,7	110,8
RO-302BO-31	391	28612	1,9	17,7716	2,1	0,6099	2,5	0,0786	1,4	0,56	487,8	6,6	483,5	9,8	463,0	46,8	487,8	6,6	105,4
RO-302BO-32	385	16770	2,3	17,8453	1,8	0,5871	3,3	0,0760	2,8	0,85	472,1	12,7	469,0	12,4	453,9	39,1	472,1	12,7	104,0
RO-302BO-33	57	2484	3,7	17,9815	12,0	0,5842	12,1	0,0762	1,6	0,13	473,4	7,2	467,2	45,5	436,9	269,1	473,4	7,2	108,3
RO-302BO-34	218	9594	2,9	18,2336	3,1	0,5523	3,6	0,0730	1,9	0,51	454,4	8,2	446,5	13,1	405,8	69,5	454,4	8,2	112,0
RO-302BO-35	501	18962	1,9	17,5479	1,3	0,5976	2,5	0,0761	2,1	0,84	472,6	9,5	475,7	9,4	491,0	29,2	472,6	9,5	96,2
RO-302BO-36	327	18908	2,7	17,7455	3,1	0,6142	3,3	0,0790	1,0	0,31	490,4	4,7	486,2	12,6	466,3	68,8	490,4	4,7	105,2